From Greenhouse to Icehouse:
The late Mesozoic-Cenozoic
Arctic Ocean Sea Ice and Climate History

by Ruediger Stein*

Abstract: Within this review paper, proxy records were used for reconstruction of the late Mesozoic-Cenozoic long-term climate history of the Arctic Ocean with a focus on sea ice and sea-surface temperature. In this context, three examples representing different climatic stages of the Arctic Ocean on its way from Greenhouse to Icehouse conditions are presented and discussed: (1) the late Cretaceous, a time interval of pre-dominantly warm climate with strong seasonality and occasionally winter sea ice, some increased paleoproductivity, and probably oxygen-deficient conditions; (2) the mid-Eocene with continuing warm and euxinic conditions and partly increased paleoproductivity, and the early onset of predominantly seasonal sea-ice conditions, and (3) the late Miocene characterized by relatively warm (SSTs of about 5 °C) and ice-free conditions during summer, as well as sea ice occurring during spring and autumn/winter.

Zusammenfassung: Der vorliegende Review-Artikel befasst sich mit der Rekonstruktion der spätmesozoisch-känozoischen langzeitlichen Klimaentwicklung des Arktischen Ozeans im Verlauf des Übergangs von Treibhaus- zu Eishausbedingungen. Der Schwerpunkt liegt dabei auf der Rekonstruktion der Änderungen von Oberflächenwassertemperaturen und Meereisverbreitung mittels bestimmter Biomarker. Herausgegriffen werden drei Beispielsituationen: (1) Die Oberkreide mit vorherrschend warmen (>15 °C) und eisfreien Klimabedingungen, z.T. erhöhter Primärproduktion und euxinischen Verhältnissen. (2) Das mittlere Eozän mit weiterhin warmen (ca. 10-25 °C) und euxinischen Bedingungen und z.T. erhöhter Primärproduktion und dem Einsetzen einer saisonalen Meereisbedeckung. (3) Das späte Miozän mit noch relativ warmen (ca. 5 °C) und eisfreien Bedingungen im Sommer aber Meereis im Winter und Frühling.

INTRODUCTION AND BACKGROUND

The sea-ice cover with its strong seasonal variability in the marginal (shelf) seas is one of the important and most obvious characteristics of the modern Arctic Ocean (Fig. 1; Thomas & Diekmann 2010). It has a large influence on the entire environment and climate of the Arctic Ocean. Sea-ice formation is strongly controlled by freshwater supply, as freshwater is essential for the maintainance of the low-salinity layer of the central Arctic Ocean. Thus, sea ice contributes significantly to the strong stratification of the near-surface water masses, encouraging sea-ice formation (e.g., Aagaard & Carmack 1989, Macdonald et al. 2004). Formation and melting of sea ice result in distinct changes in the surface albedo, the energy balance, and the temperature and salinity structure

of the upper water masses (Fig. 2). Furthermore, the sea-ice cover strongly affects the biological productivity, as a more closed sea-ice cover restricts primary production due to low light influx in the surface waters (Fig. 2). Owing to its light limitation and sea-ice cover, the central Arctic Ocean is the least productive region of the world's oceans, whereas in the marginal ice zone high primary productivity may be reached (Sakshaug 2004, Wassmann et al. 2004, Wassmann 2011). This is clearly reflected in the organic matter determined in Arctic Ocean sediments, dominated by terrigenous organic matter and a strong decrease in organic carbon accumulation towards the central Arctic Ocean basins (Fig. 3; Stein & Macdonald 2004).

The importance of Arctic sea ice goes much beyond the Arctic Ocean itself. Freshwater and sea ice are exported from the Arctic Ocean through the Fram Strait into the North Atlantic. The interplay of the cold Arctic freshwater-rich surface-water layer and its ice cover with relatively warm and saline Atlantic Water is important for the renewal of deep water driving the global thermo-haline circulation (THC) (e.g., Broecker 1997, Clark et al. 2002). Because it is involved in several key climate feedbacks (ice-albedo feedback, cloud-radiation feedback, deep-water formation, etc), sea ice plays a substantial role in climate system variability, known as "polar amplification" (Serreze & Barry 2011).

Over the last three to four decades, coinciding with global warming and atmospheric CO_2 increase, the extent and thickness of Arctic sea ice has changed dramatically (Fig. 4; Serreze et al. 2007, Stroeve et al. 2007, 2012, Cavalieri & Parkinson 2012, Stocker et al. 2013). The observed decrease in sea ice seems to be much more rapid than predicted by climate models (Fig. 4; Stroeve et al. 2007, 2012, Wang & Overland 2012). Whereas it is unquestionable that the Arctic Ocean and surrounding areas are presently subject to rapid and dramatic change, the driving forces of this change are not fully understood. Thus, a key aspect remains to distinguish and quantify more precisely the natural and anthropogenic greenhouse gas forcing of global climate change and related sea-ice decrease (Stocker et al. 2013). High-resolution paleoclimatic records going back beyond the timescale of direct observations may help to reduce some of the uncertainties in the debate of recent climate change. In this context, not only high-resolution studies of the most recent (Holocene) climate history are of importance, but also detailed studies of the earlier Earth history characterized by a much warmer (Greenhouse-type) global climate with elevated atmospheric CO_2 concentrations. A more precise knowledge of processes controlling past climate change is the only means to separate natural and anthropogenic
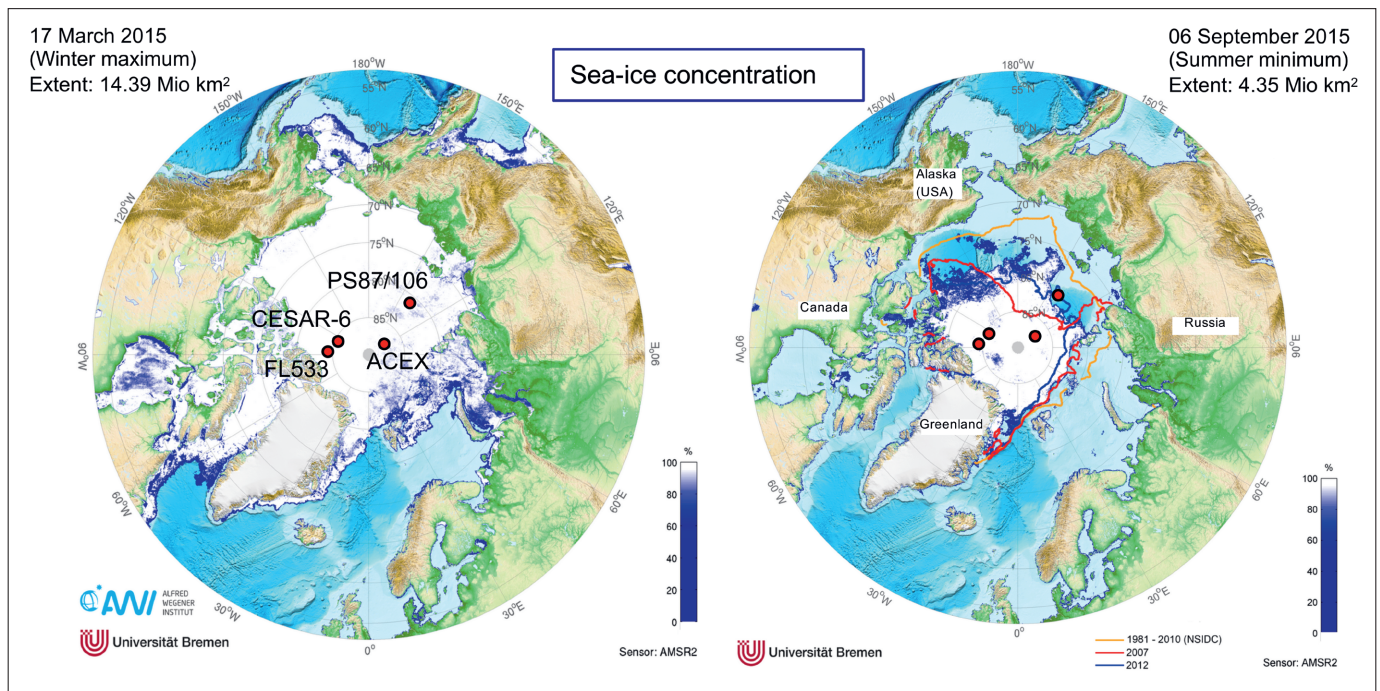
Fig. 1: Maximum and minimum sea-ice distribution in the Arctic Ocean in March (winter) 2015 and September (summer) 2015, respectively (Data source: www.meereisportal.de). Mean minimum sea-ice distribution for the period 1981-2010 and the extreme minima of 2007 and 2012 are indicated as orange, red and blue lines, respectively. Locations of the four core sites discussed in this study are shown by red circles.

Abb. 1: Maximale und minimale Meereisverbreitung im Arktischen Ozean im März (Winter) bzw. September (Sommer) 2015 (Daten: www.meereisportal.de). Mittlere minimale Meereisausbreitung im Spätsommer (September)1981-2010 sowie die extremen Meereisminima in den Jahren 2007 und 2012 sind als orange, rote bzw. blaue Linien eingetragen. Die Lokationen der hier diskutierten Sedimentkerne sind durch rote Kreise dargestellt.
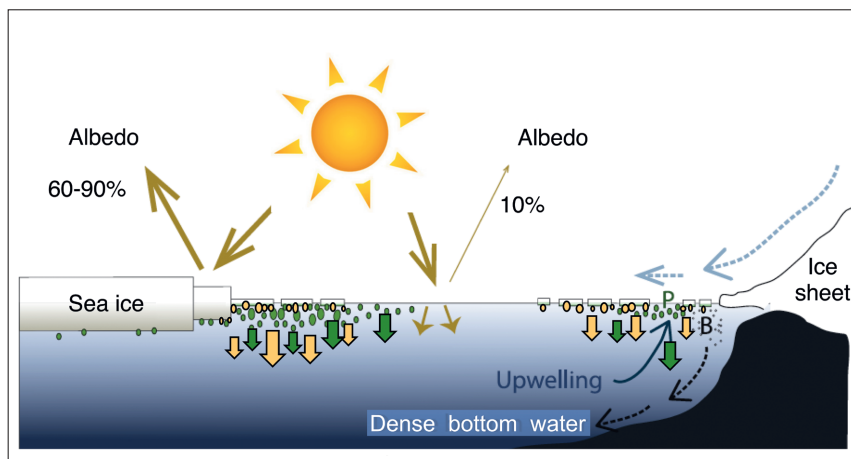

Fig. 2: Simplified scheme of the role of sea ice in the climate and ocean system, indicating the modern central and ice-edge Arctic area (left) and the glacial Arctic situation with ice sheets reaching the shelf break (right), a situation similar to the modern circum-Antarctic situation. Furthermore, solar energy (yellow-olive arrows), katabatic winds (light blue arrow), albedo effect, and ocean processes such as upwelling and brine formation (B), polynyas (P), phytoplankton production (little light green circles) and sea-ice algae (and IP$_{25}$) production (little yellow circles) with related fluxes (green and yellow arrows, respectively) are shown, (Adapted from DE VERNAL et al. (2013), supplemented.

Abb. 2: Schematische Darstellung der Rolle des Meereises im Klima- und Ozeansystem mit rezenter Situation (links) und glazialen Verhältnissen mit Eisschildvorstoß bis an die Schelfkante (rechts) für die Arktis. Die letztere (rechte) Situation entspricht in etwa den heutigen Bedingungen in der Antarktis, (nach DE VERNAL et al. (2013).

forcings and will enable us to further increase the reliability of prediction of future climate change (cf., FLATO et al. 2004, PALEOSENS Project Members 2012).

This review paper is dealing with proxy reconstructions of the late Mesozoic-Cenozoic long-term climate history of the Arctic Ocean with a focus on the sea-ice cover and sea-surface temperature (SST). During this time interval, the transition from a Greenhouse World with a warm ice-free Arctic Ocean to an Icehouse World with a cold ice-covered sea surface occurred (Fig. 5; ZACHOS et al. 2008, FRIEDRICH et al. 2012). Whereas for the low- and mid-latitudes as well as the Southern Ocean several long-term climate records are available from studies within the international DSDP-ODP-IODP program (see synthesis by STEIN et al. 2014 and references therein),

most records from the Arctic Ocean are restricted to the late Pliocene/Quaternary time interval, with a very few exceptions (Fig. 5). This includes the four short sediment cores obtained by gravity coring from drifting ice floes over the Alpha Ridge, where older pre-Neogene organic-carbon-rich muds and laminated biosiliceous oozes were sampled (JACKSON et al. 1985, CLARK et al. 1986, DAVIES et al. 2009). Most recently, a short sedimentary section representing the late Miocene (STEIN 2015, STEIN et al. 2016) was recovered. However, continuous sedimentary records from the central Arctic Ocean, allowing the development of chronologic sequences of climate and environmental change through Cenozoic times as well as a comparison with global climate records were missing prior to the IODP Expedition 302 (Arctic Ocean Coring Expedition ACEX; BACKMAN et al. 2006, MORAN et al. 2006).
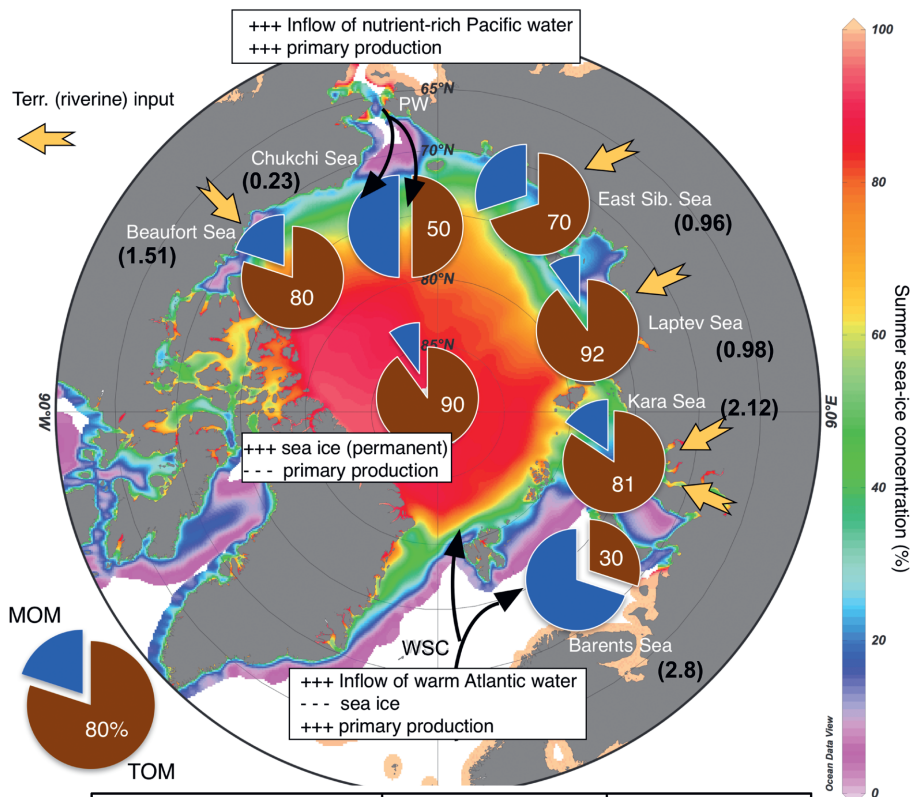
Fig. 3: Terrigenous (TOM) and marine (MOM) organic carbon in surface sediments from Arctic marginal seas and central Arctic Ocean and main processes controlling organic carbon (OC) input. In the pie diagrams, average percentage values of terrigenous (brown colour) and marine, i.e. marine/ aquatic and ice algae (blue colour), are given. In addition, OC accumulation rates for the different Arctic Ocean areas (table) and the Arctic marginal seas (bold numbers in brackets) are listed. For data base see STEIN & MACDONALD (2004), STEIN (2008), and references therein. Colour bar in the right indicates average summer sea-ice concentrations (1988-2007) shown in the map (Source data: NSIDC).

Abb. 3: Anteile von terrigenem (TOM, braune Signatur) und marinem (MOM, blaue Signatur) organischen Kohlenstoff (OC) in Oberflächensedimenten des zentralen Arktischen Ozeans und der angrenzenden Randmeere sowie Hauptsteuerungsprozesse für den OC-Eintrag. Zusätzlich sind die Akkumulationsraten für die unterschiedlichen Gebiete angegeben (Daten: STEIN & MACDONALD 2004, STEIN 2008). Farbskala mit Zahlenwerten 0-100 an der rechten Bildseite gibt Prozentwerte für die in der Karte dargestellten sommerlichen Meereisverbreitungen (1988-2007; NSIDC).

Area	Size (10^3 km^2)	OC (10^6 t y^{-1})
Continental shelves	5052	8.68
Continental Slopes	541	1.29
Continental rises	1095	0.72
Abyssal plains	1367	0.25
Ridges	1506	0.11
Total Arctic	**9555**	**11**

Approaches for reconstruction of past sea-ice conditions and sea-surface temperatures

A large number of studies dealing with the reconstruction of past sea-ice cover are based on sedimentological, mineralogical, and geochemical data (e.g., KNIES et al. 2000, NØRGAARD-PEDERSEN et al. 2003, SPIELHAGEN et al. 2004, DARBY 2008, POLYAK et al. 2010), as well as microfossils such as diatoms, dinoflagellates, ostracods, and foraminifers (e.g., KOÇ et al. 1993, MATTHIESSEN et al. 2001, 2009, POLYAK et al. 2010, CRONIN et al. 2013, DE VERNAL et al. 2013). If used as a single proxy these parameters have major disadvantages. Coarse-grained terrigenous particles, i.e., ice-rafted debris (IRD) indicative for transport by ice, do not always allow to distinguish between transport by sea ice or icebergs. Specific sea-ice associated organisms like pennate ice diatoms and ostracods are frequently used for reconstructing present and past sea-ice conditions (e.g., KOÇ et al. 1993, STICKLEY et al. 2009, CRONIN et al. 2013). However, it has also been shown that the preservation of fragile siliceous diatom frustules can be relatively poor in sediments from the Arctic realm and the same is also true (if not worse) for calcareous-walled microfossils, thus limiting their applicability (e.g., STEINSUND & HALD 1994, MATTHIESSEN et al. 2001).

The ability to (semi-)quantitatively reconstruct paleosea-ice distributions has been significantly improved by a biomarker approach based on determination of a highly branched isoprenoid (HBI) with 25 carbons (C_{25} HBI monoene = IP_{25}) (Fig. 6; BELT et al. 2007). This biomarker is only biosynthesized by specific diatoms living in the Arctic ice (Fig. 6; BROWN et al. 2014), meaning the presence of IP_{25} in the sediment is a direct proof of the presence of past Arctic sea ice. Furthermore, it appears to be a specific, sensitive and stable proxy for Arctic sea ice in sedimentary sections representing late Miocene to Holocene times (STEIN et al. 2012, 2016, BELT & MÜLLER 2013 and references therein). When using this proxy one has to consider that IP_{25} is absent under a permanent sea-ice cover limiting light penetration and, in consequence, sea-ice algal growth (i.e. $IP_{25} = 0$). The same consequence applies to totally ice-free conditions where no ice algae live. This difficulty in interpretating IP_{25} data can be overcome by the additional use of phytoplankton-derived, open water biomarkers such as brassicasterol and dinosterol (MÜLLER et al. 2009, 2011) or a specific tri-unsaturated HBI (BELT et al. 2015, SMIK et al. 2016). By combining the environmental information carried by IP_{25} and phytoplankton biomarkers in a phytoplankton-IP_{25} index, the so-called "PIP_{25} index", even more semi-quantitative estimates of present and past sea-ice coverage are possible (for details see MÜLLER et al. 2011, BELT et al. 2015, SMIK et al. 2016).
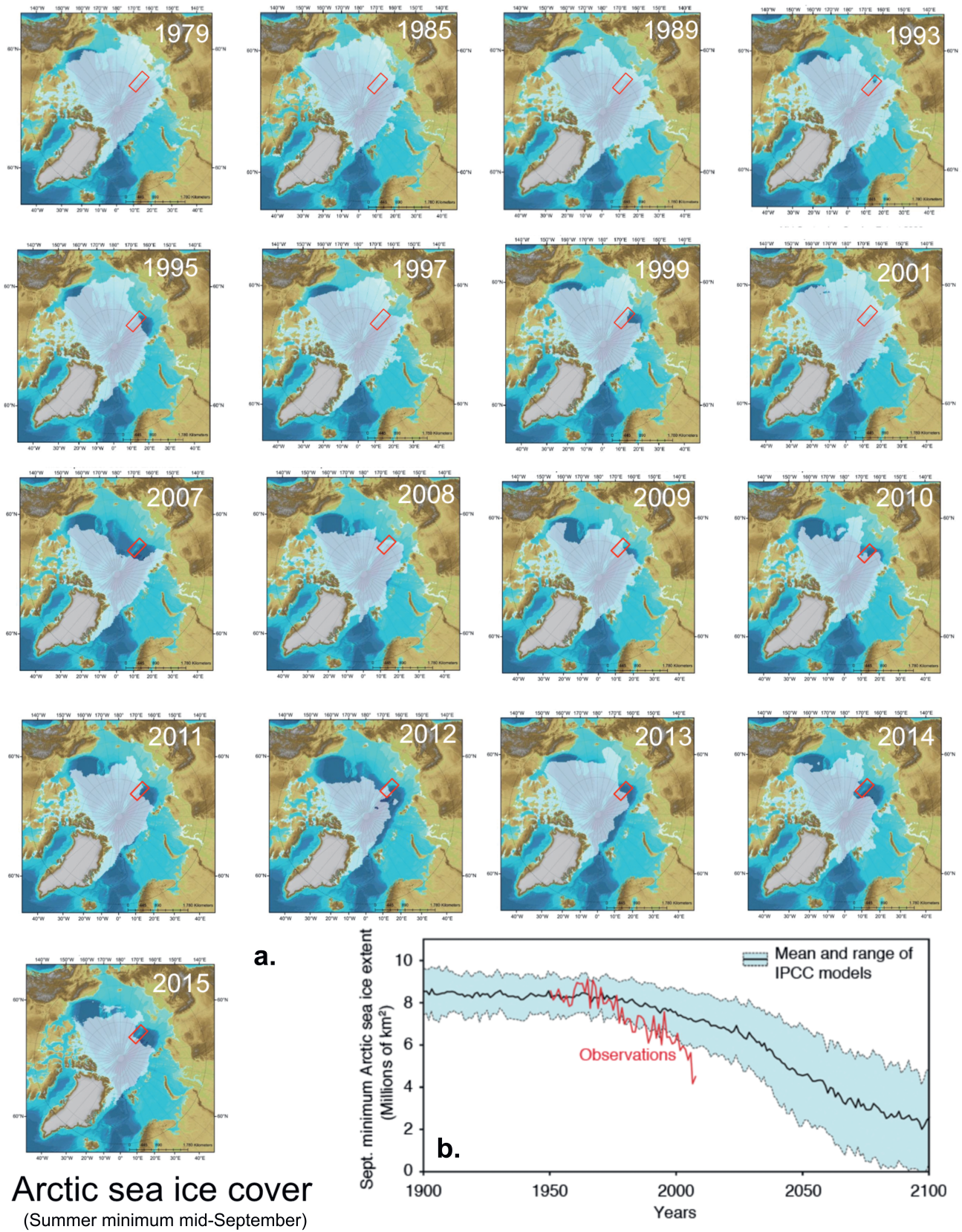
Arctic sea ice cover
(Summer minimum mid-September)

Fig. 4: (**a**): Mid-September (summer minimum) Arctic sea-ice extent for selected years between 1979 and 2015 (Data source: PENG et al. 2013). Red rectangle indicates work area of PS87 site survey (cf. fig. 14). (**b**): Mean and range of Arctic September sea-ice extents (x 10⁶ km²) from different IPCC (Intergovernmental Panel on Climate Change) climate models (multi-model mean displayed as bold black line) and observations (red line) (STROEVE et al. 2007, 2012).

Abb. 4: (**a**) Minimale Meereisverbreitung im Arktischen Ozean im September für ausgewählte Jahre zwischen 1979 und 2015 (Datenquelle: PENG et al., 2013). Rotes Rechteck zeigt das Arbeitsgebirt der Expedition PS87.(**b**) Meereisausdehnung im Arktischen Ozean für September (in 10⁶ km²) für die Zeit 1900 bis 2100, dargestellt als Mittelwerte der Ergebnisse unterschiedlicher IPCC-Klimamodelle (fett-schwarze Kurve) mit Standardabweichung (grauer Bereich). Zusätzlich sind Beobachtungen und Messwerte für den Zeitraum von ca. 1950-2010 angegeben (rote Kurve). Datenquelle: STROEVE et al. 2007, 2012.
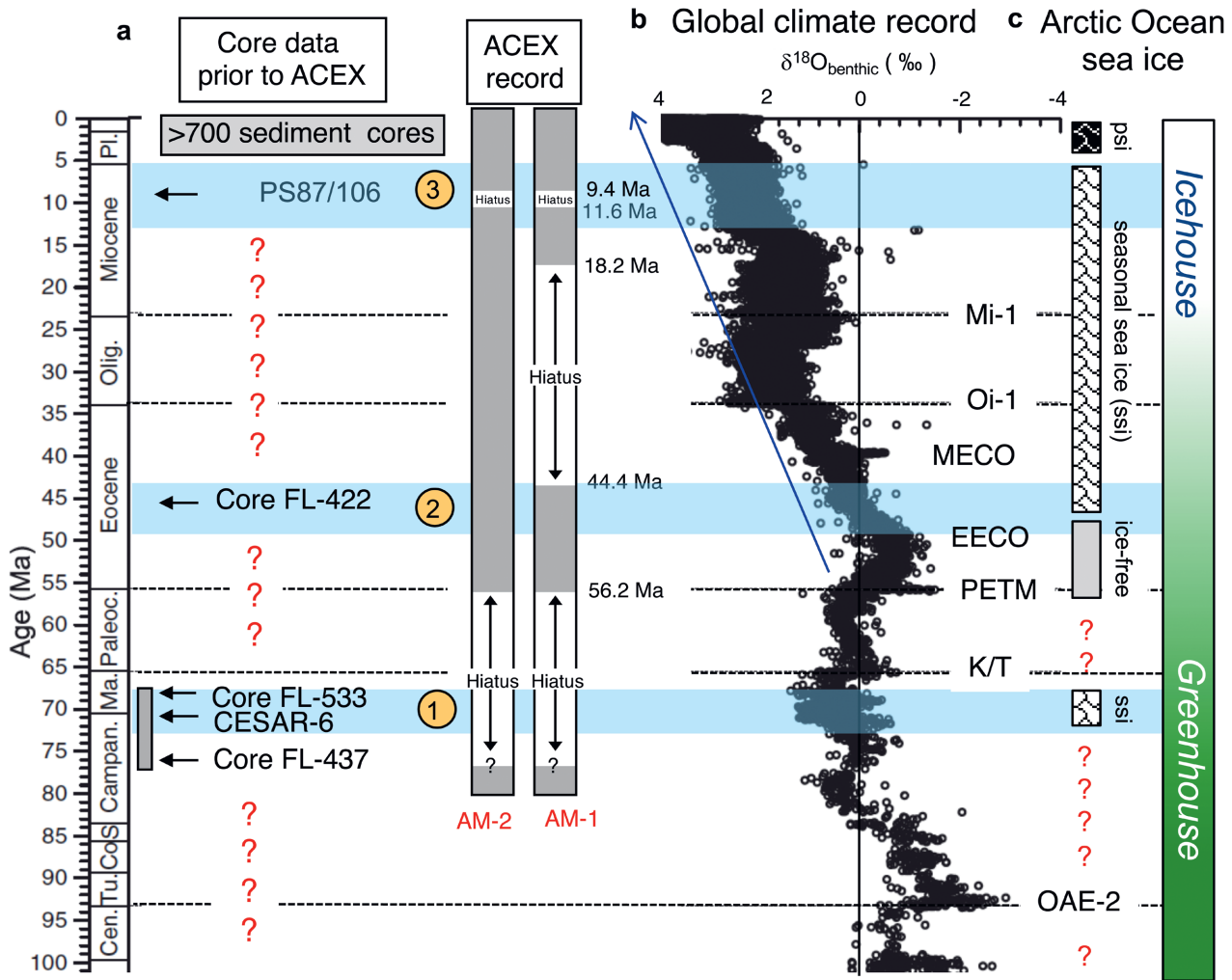
Fig. 5: Stratigraphic coverage of existing sediment cores in the central Arctic Ocean prior to IODP-ACEX (2004), including the four short cores representing short sections of Eocene and/or Maastrichtian/Campanian sediments (THIEDE et al. 1990, BACKMAN et al. 2008, STEIN et al. 2015) and one core representing late Miocene sediments (STEIN 2015, STEIN et al. 2016), and the section recovered during the ACEX drilling expedition with age models of BACKMAN et al. (2008) (AM-1) and POIRIER & HILLAIRE-MARCEL (2011) (AM-2). Large yellow circles with numbers 1 to 3 indicate time intervals discussed in this paper. (b) Global $\partial^{18}O$ stack of benthic foraminifera for the past 100 million years representing the Greenhouse-Icehouse transition (FRIEDRICH et al. 2012). C/T = Cenomanian/Turonian boundary; C/P = Cretaceous/Paleogene Boundary; PETM = Paleocene-Eocene Thermal Maximum; EECO = Early Eocene Climate Optimum; MECO = Middle Eocene Climate Optimum; Mi-1 = Major Miocene glaciation event; Oi-1 = Major Oligocene glaciation event. (c) Occurrence of perennial sea ice (psi), seasonal sea ice (ssi), and ice-free conditions during the last about 100 Ma as proposed in this paper. Red questionmarks indicate no information on sea ice available.

Abb. 5: (a) Zeitliche Einstufung der vorhandenen Sedimentkerne aus dem Arktischen Ozean vor Durchführung der IODP-Bohrung (ACEX 2004, THIEDE et al. 1990, BACKMAN et al. 2008, STEIN et al. 2015, 2016) sowie stratigraphische Reichweite der ACEX-Bohrung nach Altersmodell AM-1 (BACKMAN et al. 2008) und Altersmodell AM-2 (POIRIER & HILLAIRE-MARCEL 2011). Die Nummern 1 bis 3 markieren die Zeitintervalle, die in dieser Arbeit diskutiert werden. **(b)** Globale $\partial^{18}O$-Kurve von benthischen Foraminiferen, welche die langzeitliche Abkühlung und den Wechsel von Treibhaus- zu Eishausbedingungen im Verlauf der letzten 100 Millionen Jahre vor Heute anzeigen (FRIEDRICH et al. 2012). **(c)** Zeitintervalle mit ganzjähriger Meereisbedeckung (psi), saisonaler Meereisbedeckung (ssi), und eisfreien Bedingungen in der zentralen Arktis (diese Arbeit). Rote Fragezeichen markieren Zeitintervalle mit fehlenden Daten zur Meereisverbreitung an.

Another useful approach that helps to distinguish between the two "IP$_{25}$ = 0" extremes, i.e., ice-free *versus* thick closed ice coverage, is the determination of sea-surface temperature (SST). SST values significantly above 0 °C give important information about surface water characteristics per se, but also clearly point to ice-free conditions if IP$_{25}$ = 0. For SST reconstructions, transfer function techniques based on microfossil assemblages (e.g., PFLAUMANN et al. 2003) and Mg/Ca ratios (e.g., LEAR et al. 2000) as well as very promising biomarker SST tools such as the alkenone-based U^{K}_{37} index (BRASSELL et al. 1986, PRAHL & WAKEHAM 1987) and the Tex$_{86}$ index (SCHOUTEN et al. 2002, 2004) are available. These two biomarker SST tools are also used in this paper (Fig. 6).

The alkenone-based U^{K}_{37} approach evolved from the observation that certain microalgae of the class Prymnesiophyceae, notably the marine coccolithophorids *Emiliania huxleyi* and *Gephyrocapsa oceanica* (e.g., VOLKMAN et al. 1980, MARLOWE et al. 1984, CONTE et al. 1992), and presumably other living and extinct members of the family Gephyrocapsae (MARLOWE et al. 1990, MÜLLER et al. 1998), have or had the capability to synthesize alkenones whose extent of unsaturation changes with growth temperature (Fig. 6; MARLOWE et al. 1984, BRASSELL et al. 1986, PRAHL & WAKEHAM 1987). Based on this correlation, paleo-SST can be calculated from the so-called ketone unsaturation index U^{K}_{37} (BRASSELL et al. 1986, PRAHL & WAKEHAM 1987, MÜLLER et al. 1998) or the simplified version of the index U^{K}_{37}' (Fig. 6; PRAHL & WAKEHAM 1987, MÜLLER et al. 1998).
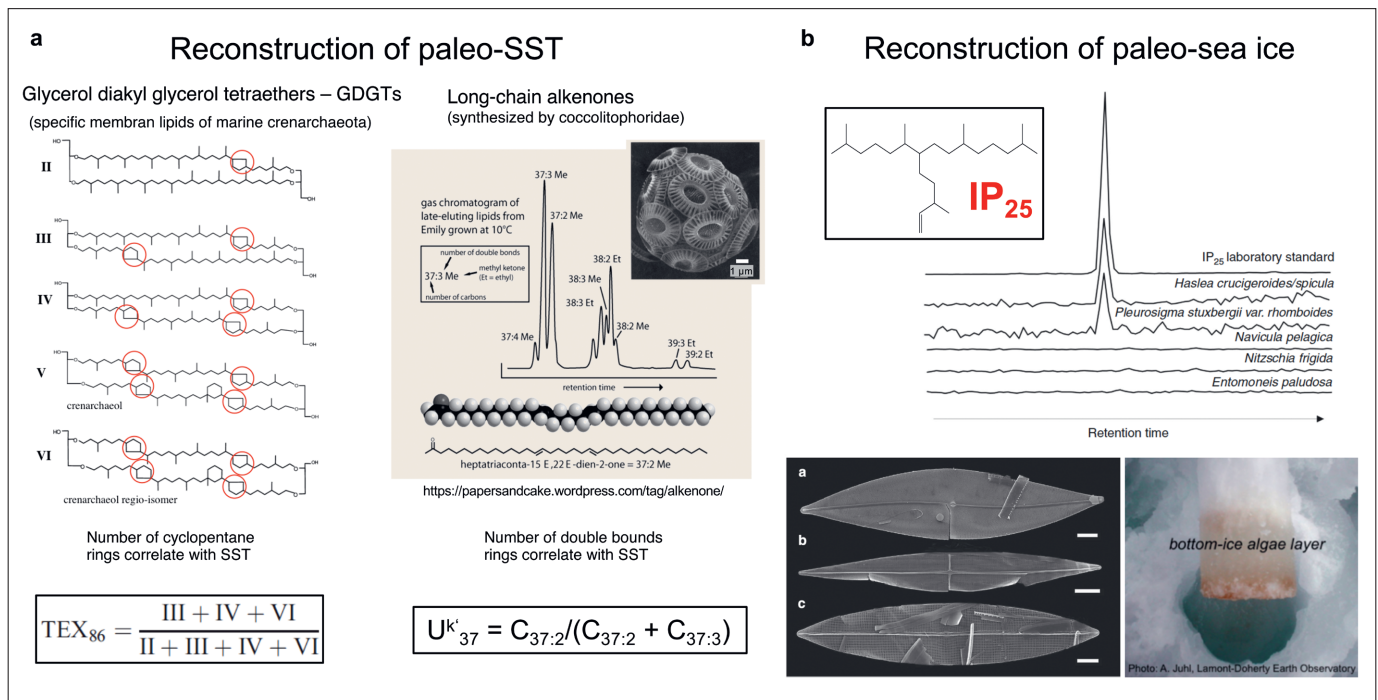
a Reconstruction of paleo-SST

Glycerol diakyl glycerol tetraethers – GDGTs
(specific membran lipids of marine crenarchaeota)

II
III
IV
V
crenarchaeol
VI
crenarchaeol regio-isomer

Number of cyclopentane
rings correlate with SST

$$TEX_{86} = \frac{III + IV + VI}{II + III + IV + VI}$$

Long-chain alkenones
(synthesized by coccolithophoridae)

gas chromatogram of
late-eluting lipids from
Emily grown at 10°C

number of double bonds
37:3 Me ← methyl ketone
(Et = ethyl)
number of carbons

37:4 Me   37:3 Me   37:2 Me   38:2 Et   38:3 Me   38:3 Et   38:2 Me   39:3 Et   39:2 Et

retention time

1 µm

heptatriaconta-15 E,22 E -dien-2-one = 37:2 Me

https://papersandcake.wordpress.com/tag/alkenone/

Number of double bounds
rings correlate with SST

$$U^{k'}_{37} = C_{37:2}/(C_{37:2} + C_{37:3})$$

b Reconstruction of paleo-sea ice

IP₂₅

IP₂₅ laboratory standard
Haslea crucigeroides/spicula
Pleurosigma stuxbergii var. rhomboides
Navicula pelagica
Nitzschia frigida
Entomoneis paludosa

Retention time

a   b   c

bottom-ice algae layer

Photo: A. Juhl, Lamont-Doherty Earth Observatory

Fig. 6: Biomarker proxies used for reconstruction of (**a**): sea-surface temperatures (TEX$_{86}$-Index: SCHOUTEN et al. 2002, U$^{k'}_{37}$-Index: BRASSELL et al. 1986, PRAHL & WAKEHAM 1987) and (**b**): sea ice (IP$_{25}$) (BELT et al. 2007, BROWN et al. 2014).

Abb. 6: Biomarker-Proxys für die Rekonstruktion der (**a**): Oberflächenwassertemperatur (TEX$_{86}$-Index: SCHOUTEN et al. 2002, U$^{k'}_{37}$-Index: BRASSELL et al. 1986, PRAHL & WAKEHAM 1987) und (**b**): von Meereis (IP$_{25}$) (BELT et al. 2007, BROWN et al. 2014).

Furthermore, the C_{37} tetra-unsaturated alkenone ($C_{37:4}$) seems to be enriched in cold low-salinity waters. Salinity perturbations in the northern North-Atlantic related to periods of massive ice and iceberg melting during Heinrich-type IRD events, for example, are reflected in the occurrence and relative abundance of $C_{37:4}$, as shown in studies of several North Atlantic sediment cores (e.g., ROSELL-MELÉ 1998, BARD et al. 2000, ROSELL-MELÉ et al. 2002, SICRE et al. 2002, STEIN et al. 2009, 2014). Thus, this approach, i.e., the relative abundance of $C_{37:4}$, might be a first-order proxy for the identification of meltwater influence in a sedimentary record.

The TEX$_{86}$ approach is based on specific membrane lipids, i.e., tetraether lipids (glycerol diakyl glycerol tetraethers, GDGTs) with 0-4 cyclopentane rings and, in one case, a cyclohexane ring (for molecular structures see Fig. 6), synthesized by marine Crenarchaeota (SCHOUTEN et al. 2002). As shown in a study of marine surface sediments from the world oceans, these organisms adjust the composition of their tetraether membranes lipids in response to SST (SCHOUTEN et al. 2002, 2004, WEIJERS et al. 2006). This response is quantified as the so-called TEX$_{86}$ (tetraether index of 86 carbon atoms). For further detailed discussion of strengths and limits of the TEX$_{86}$ approach the reader is referred to SCHOUTEN et al. (2002, 2004), WUCHTER et al. (2004), WEIJERS et al. (2006), and HO et al. (2014).

In this paper, the reconstruction of the long-term Arctic Ocean sea ice and climate history is mainly based on organic-geochemical (biomarker) proxies: HBIs including IP$_{25}$ (indicative for sea ice and phytoplankton), sterols (indicative for phytoplankton and terrigenous higher plants), long-chain n-alkanes (indicative for higher-plant input), alkenones (indicative for phytoplankton, SST and salinity/meltwater discharge), and GDGTs (indicative for SST) as well as the total organic carbon (OC) content as general proxy for environmental information (productivity, oxygenation of water masses, etc.).

THE LONG-TERM ARCTIC OCEAN SEA ICE AND CLIMATE HISTORY: RECONSTRUCTIONS BASED ON BIOMARKER PROXIES

The long-term late Mesozoic – Cenozoic paleoclimatic and paleoceanographic history of the Arctic Ocean remains still poorly known compared to other world ocean areas. Major information on the paleoenvironment of the early Arctic is derived from petroleum exploration drill holes from the Arctic marginal seas as well as DSDP and ODP drill cores from sub-arctic regions (see reviews by STEIN 2008, STEIN et al. 2014, 2015 for references). Direct information from sediment cores derived from the central Arctic Ocean, however, are restricted to a very few short sections, at least prior to the IODP-ACEX drilling campaign in 2004 (Fig. 5). Here, due to the limited data base, three examples representing different climatic stages of the Arctic Ocean on its way from Greenhouse to Icehouse conditions are presented in Figure 5 and discussed: (1) the late Cretaceous, (2) the Eocene, and (3) the late Miocene.

The central Arctic Ocean during late Cretaceous times

In the central Arctic Ocean, Cretaceous sediments were only cored from three locations on the Alpha Ridge: cores Fl-437 and Fl-533 taken during the drift of the ice-island T-3 from

1963 to1974 and Core CESAR-6 of the Canadian Expedition to Study the Alpha Ridge (CESAR) in 1983 (see Fig. 7a for core locations). In 2004, an about 3 m thick interval of Campanian very dark gray clayey mud and silty sands with OC values of about 1-2 % was recovered in the lowermost part of the ACEX record (BACKMAN et al. 2006, STEIN 2007).

At site CESAR-6, siliceous sediments with excellently preserved microfossils were retrieved. These sediments are well-laminated (Fig. 7b) and contain variable amounts of iron and manganese that impart a characteristic dark pigment to some laminae, organic carbon contents are typically <1 % (JACKSON et al. 1985). The age attribution of this core includes the interval Campanian-Maastrichtian, depending on whether diatoms, silicoflagellates or palynomorphs are taken as the prime biostratigraphic indicator (JACKSON et al. 1985). Very similar sediments of Campanian age were also recovered at site Fl-437: a yellowish laminated siliceous ooze rich in
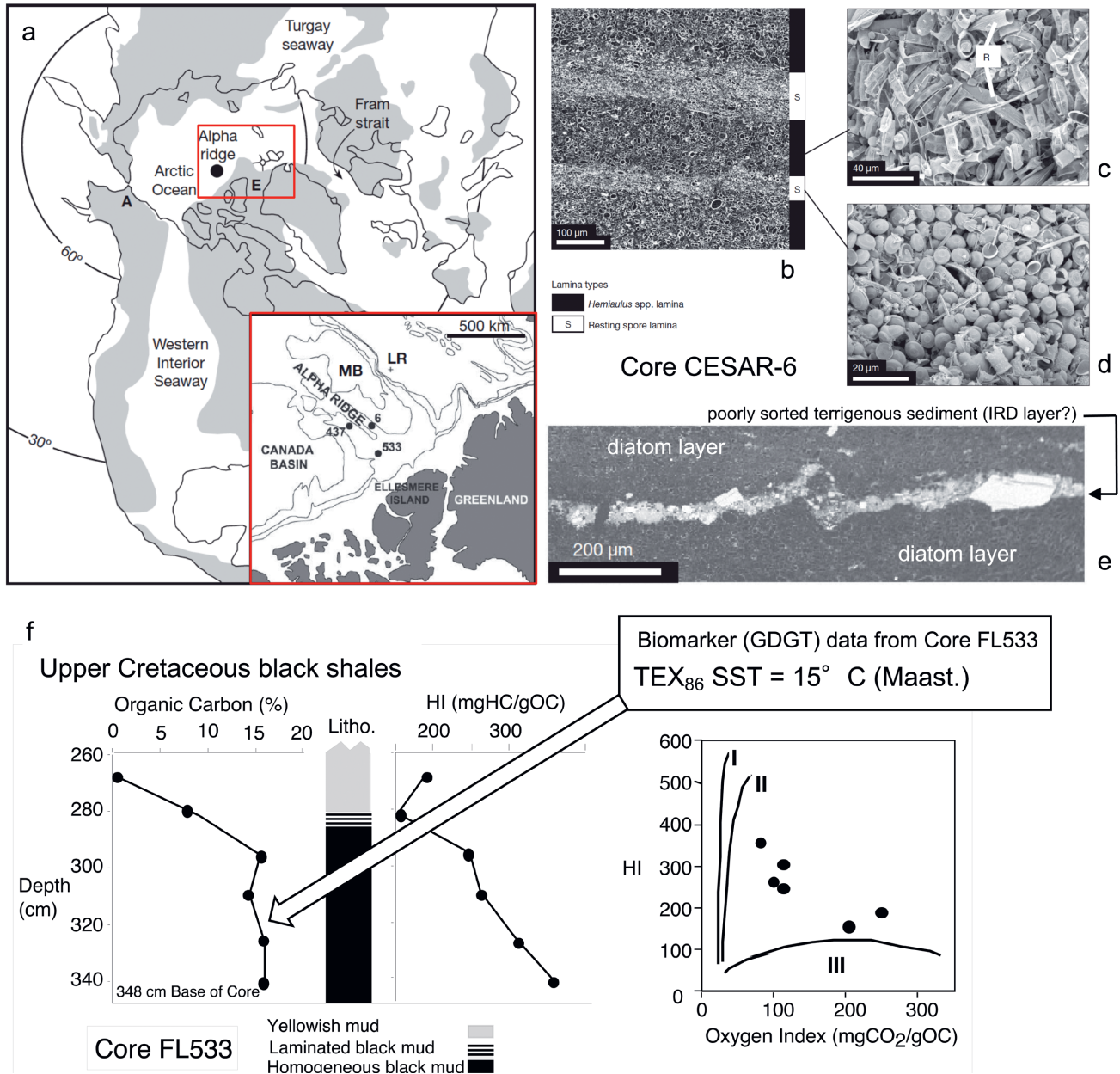

Core CESAR-6

Biomarker (GDGT) data from Core FL533
TEX_{86} SST = 15° C (Maast.)

Core FL533

Fig. 7: (**a**): Map showing the late Cretaceous paleogeography of the Arctic region with the Alpha Ridge; inset shows modern geography and location of the Alpha Ridge cores CESAR-6, FL-37 and Fl-533. LR: Lomonosov Ridge, MB: Makarov Basin. (**b**): Back Scattered Electron Image of resin-embedded sediment showing darker diatom vegetative cell laminae, interbedded with paler layers composed primarily of diatom resting spores (scale bar 100 μm). Representative topographic SEM images of (**c**): diatom vegetative cells and (**d**): diatom resting spores (scale bar 20 microns). (**e**): Thin laminae of poorly sorted terrigenous sediment occurring dominantly within the spring diatom bloom layer, interpreted as evidence for ice rafting (scale bar 200 μm). (**f**): Organic carbon, hydrogen index and oxygen index data and lithologies of the lowermost upper Cretaceous section of Core FL-533 (data from CLARK et al. 1986, FIRTH & CLARK 1998). TEX_{86} SST from JENKYNS et al. (2004). (**a**): to (**e**): from DAVIES et al. (2009) supplemented.

Abb. 7: (**a**): Karte mit Paläogeographie der Arktis-Region während der Oberkreide; kleine Karte rechts gibt Ausschnitt mit heutiger Geographie der Region um den Alpha-Rücken und Lokationen der hier diskutierten Sedimentkerne wider. (**b**) – (**e**) : Dünnschliffaufnahmen von Proben aus Kern CESAR-6 mit unterschiedlichen Diatomeen-Vergesellschaftungen bzw. -lagen und terrigener Sedimentlage (IRD). (**a**) bis (**e**): aus DAVIES et al. (2009), ergänzt. (**f**) Organischer Kohlenstoffgehalt sowie Wasserstoffindex (HI) und Sauerstoffindex (OI) in von Kern FL533 (Daten: CLARK et al. 1986, FIRTH & CLARK 1998); Tex_{86}-Temperatur aus JENKYNS et al. (2004).

diatoms, ebrideans, silicoflagellates, and archaeomonads with sparse fish remains (CLARK et al. 1986, DELL'AGNESE & CLARK 1994).

More recently, DAVIES et al. (2009, 2011) analysed in detail the laminated section of Core CESAR-6 using "Back Scattered Electron Imagery" (Figs. 7b to 7e). In their study, these authors identified a seasonal succession of two distinct lamina types that represent an annual lamina couplet. Type A of laminae consists of diatom resting spores (Fig. 7c) representing flux from the spring bloom, and Type B of laminae consists of diatom vegetative cells (Fig. 7d) representing flux from production during the stratified months of the Arctic summer (DAVIES et al. 2011). In some of these lamina couplets, coarse-grained terrigenous particles indicative of ice-rafting (IRD), were found (Fig. 7e). The diatom laminae point to a strong seasonality, i.e., to ice-free summers whereas the presence of IRD is interpreted as signal for sea ice that occasionally may have occurred during severe winters (DAVIES et al. 2009, 2011).

In Core Fl-533, the lowermost 67 cm of the 348 cm long sequence comprise OC-rich black mud (black shales) of early Maastrichtian age (FIRTH & CLARK 1998). These black shales are characterized by very high OC contents of up to almost 16 %, hydrogen index values of about 250 to 350 mgHC/gOC (Fig. 7f), and T_{max} values of about 420 °C (CLARK et al. 1986) indicating an immature, mixed marine-terrigenous type of organic matter. Whether these black shales recovered in Core FL-533 resulted from anoxic conditions in an isolated local basin, a depositional environment under an oceanic water mass exhibiting an oxygen minimum, rapid burial and/or high terrigenous OC input remains an open question. In any case, both organic carbon content and composition were totally different in comparison to those within the Quaternary deposits (Fig. 8; STEIN et al. 2001). Whereas during the Quaternary the buried OC is mainly refractory terrigenous OC, the Cretaceous OC consists to a major amount of labile algae-type OC. These estimates suggest that the Cretaceous Arctic Ocean basin may have been an important sink for algae-type OC (and CO_2) and, thus, of importance for the global climate system of that time.

JENKYNS et al. (2004) analysed samples of the black shale from Core Fl-533 for membrane lipids of marine Crenarchaeota to determine the TEX_{86} (cf., SCHOUTEN et al. 2002). This biomarker approach may allow to estimate mid-Cretaceous central Arctic Ocean sea-surface temperature (SST) more quantitatively. The TEX_{86} results indicate an average Arctic Ocean (80° N) SST of 15 +/-1 °C for that part of the early Maastrichtian represented by the black muds (Fig. 7f). Considering the diatom and IRD data from the CESAR-6 Core (see above), this SST of about 15 °C should certainly represent summer conditions. A summer SST of about 15 °C and the presence of sea ice during winter may represent conditions similar to those described for the Eocene central Arctic Ocean (see below). Comparing this high-latitude value with Maastrichtian SST values determined in the equatorial Pacific reaching 27-32 °C (WILSON & OPDYKE 1996), suggests a Northern Hemisphere pole-equator temperature gradient of about 15 °C.

The central Arctic Ocean during mid-Eocene times

With the first Mission Specific Platform (MSP) expedition within IODP in 2004 (i.e., IODP Expedition 302, ACEX), scientific drilling in the permanently ice-covered central Arctic Ocean was carried out for the first time, penetrating 428 m of Upper Cretaceous to Quaternary sediments on the crest of Lomonosov Ridge between 87° and 88° N (Fig. 9a; BACKMAN et al. 2006, 2008, MORAN et al. 2006). These sediments are characterized by prominent changes in sediment composition and texture, suggesting drastic paleoenvironmental changes through time (BACKMAN et al. 2006, STEIN 2007). Whereas the lower half of the ACEX sequence (Units 2 to 4) mainly
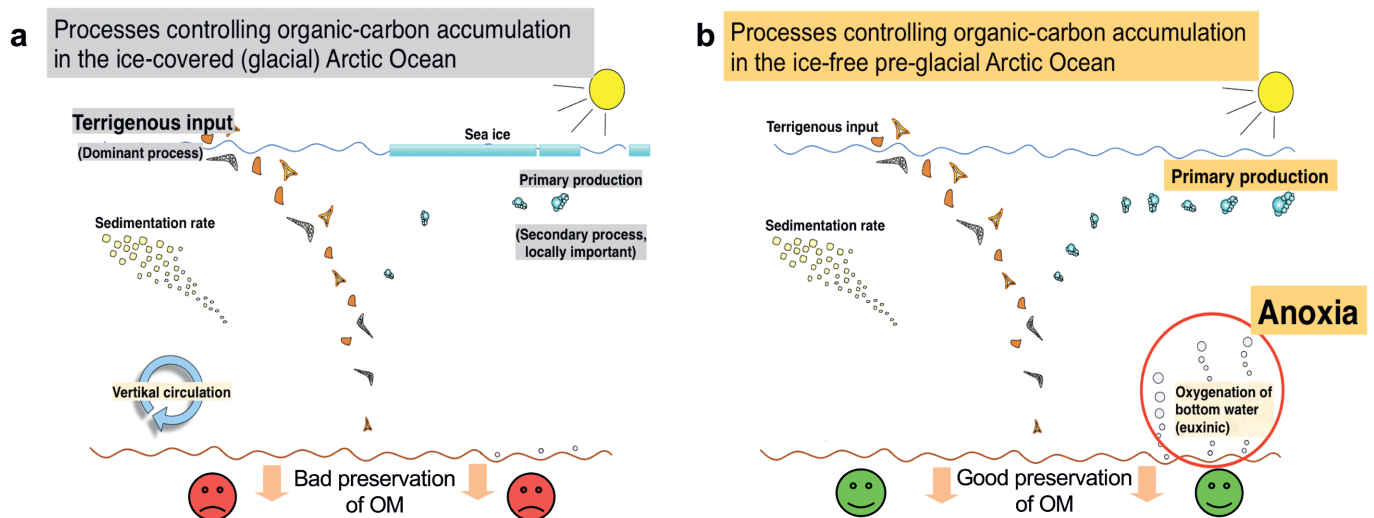

Fig. 8: Cartoon summarizing main processes controlling organic-carbon flux and accumulation in the (**a**): late Cenozoic ice-covered cold Arctic Ocean and (**b**): late Cretaceous/early Cenozoic dominantly ice-free warm Arctic Ocean.

Abb. 8: Skizze mit den Hauptprozessen, die Fluss und Akkumulation von organischem Kohlenstoff im Arktischen Ozean beeinflussen. (**a**): spätkänozoischer eisbedeckter kalter Ozean; (**b**): spätkretazischer/frühkänozoischer hauptsächlich eisfreier warmer Ozean.
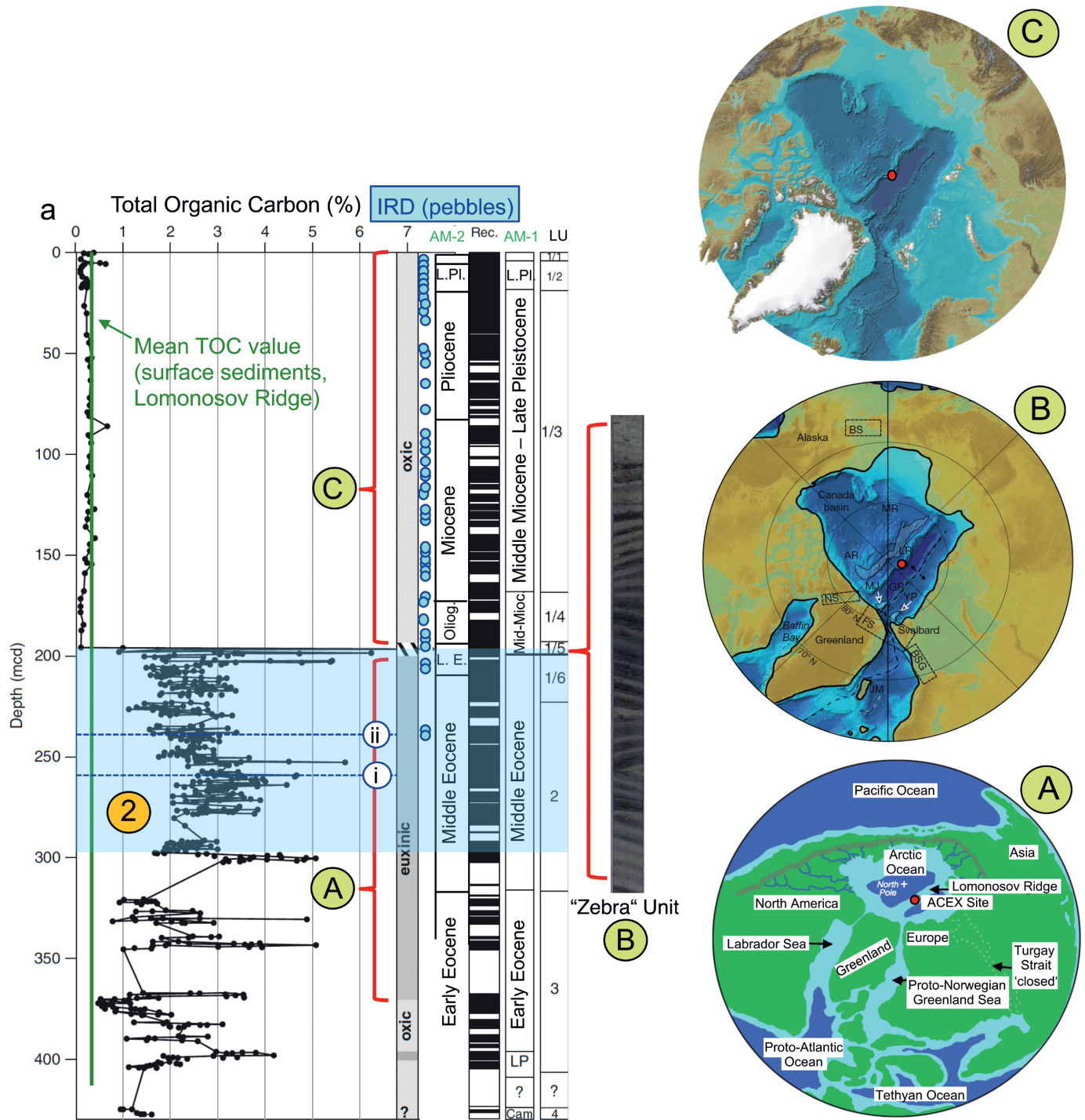
Fig. 9a: Record of total organic carbon (TOC) contents as determined in the composite ACEX sedimentary sequence (STEIN 2007). Data on lithological units (LU) and core recovery (Rec.) from BACKMAN et al. (2006). Age models AM-1 (BACKMAN et al. 2008) and AM-2 (POIRIER & HILLAIRE-MARCEL 2011) are shown. The "Zebra" Unit (Unit 1/5) marks the transition from an euxinic ocean to an oxygenated ocean that occurred when the formerly isolated Arctic Ocean became connected to the world ocean via Fram Strait. Depending on the age model, this transition is in the mid-Miocene (17.5 Ma) or Oligocene (32 Ma). Blue circles mark occurrence of pebble-sized ice-rafted debris (IRD) (ST. JOHN 2008). The light blue interval (2) with events (i) and (ii) highlight interval shown in Fig. 10. Cam = Campanian; LP = late Paleocene; Mid Mioc. = lower Miocene; L.Pl. = late Pleistocene. (**9C**): International Bathymetric Chart of the Arctic Ocean (JAKOBSSON et al. 2012) representing modern boundary conditions with connections to the world ocean. (**9B**): Paleogeographic/paleobathymetric reconstruction for the late early Miocene. BSG: Barents Sea Gateway, JM: Jan Mayen Microcontinent, KR: Knipovich Ridge, MJ: Morris Jessup Rise, NS: Nares Strait, YP Yermak Plateau (JAKOBSSON et al. 2007, supplemented). (**9A**): Paleogeography of the Arctic region for the early middle Eocene during the phase of biosilica production and preservation and euxinic conditions (50-45 Ma) (STICKLEY et al. 2009).

Abb. 9a: Organischer Kohlenstoffgehalt (TOC) der ACEX-Sedimentabfolge (Stein 2007). Lithologische Einheiten (LU) und Kerngewinn (Rec.) von BACKMAN et al. (2006) sowie Altersmodelle AM-1 (BACKMAN et al. 2008) und AM-2 (POIRIER & HILLAIRE-MARCEL 2011). Die „Zebra"-Unit (Unit 1/5) markiert den Übergang von euxinischen zu oxischen Bedingungen. Je nach Altersmodell war dieser Übergang im mittleren Miozän (17.5 Ma) oder bereits im Oligozän (32 Ma). Blaue Kreise markieren das Vorkommen von grobkörnigem (>1 cm) IRD (ST. JOHN 2008). Das hellblau markierte Interval (2) mit den Events (i) und (ii) wird in Abb. 10 detaillierter diskutiert. Cam: Kampan, LP: oberes Paläozän, Mid Mioc.: mittleres Miozän, L.Pl.: oberes Pleistozän. (**9C**): „International Bathymetric Chart of the Arctic Ocean" (JAKOBSSON et al. 2012). (**9B**): Paläogeographische/paläobathymetrische Rekonstruktion für das Miozän (JAKOBSSON et al. 2007, ergänzt). (**9A**): Paläogeographie der Arktischen Region für das frühe mittlere Eozän (50-45 Ma) (STICKLEY et al. 2009).

consists of dark gray silty clay and biosiliceous ooze characterized by high TOC values of 1 to >5 %, the upper half of the ACEX sequence (Subunits 1/1 to 1/4) is composed of silty clay with very low TOC contents of <0.5 % (Fig. 9a), i.e., values very similar to those known from upper Quaternary records determined in gravity cores from the Lomonosov Ridge and representing modern-type oxic deep-water conditions (STEIN et al. 2001). In Subunit 1/5 (about 193 to 199 m of composite depth (mcd)) characterized by distinct gray/black colour bandings ("Zebra Unit"), TOC maxima of 7 to 14.5 % were measured (Fig. 9a; STEIN 2007). The Eocene section (about 200 to 385 mcd) characterized by high (algea-type) organic carbon content are mainly related to euxinic conditions predominent at that time when the Arctic Ocean was quite isolated from the world ocean (Figs. 8, 9b; BACKMAN et al. 2006, STEIN et al. 2006, 2014). The transition from euxinic conditions to the modern-type oxic conditions occurred during Oligocene-Miocene times and is related to the opening of Fram Strait allowing the inflow of oxygen-rich deep water from the Atlantic into the Arctic Ocean (Fig. 9b JAKOBSSON et al. 2007). Across this transition, also the abundance of coarse-grained pebble-sized IRD significantly increased, being then typical in the upper half of the ACEX sequence throughout (Fig. 9a). The exact timing of this prominent environmental change, i.e., 17.5 Ma *versus* 32 Ma, however, is still under controversal discussion and depends on the age model that is used (Fig. 9a), i.e., BACKMAN et al. (2008) *versus* POIRIER & HILLAI-

RE-MARCEL (2011). The choice of the age model, of course, would also affect reconstructions of the early onset of sea ice in the Arctic Ocean during the Eocene, discussed in the following.

Prior to ACEX, it has been indirectly inferred from sub-Arctic ice-rafted debris records in the Norwegian-Greenland Sea, Iceland Sea, and Irminger Sea and Fram Strait area that the Northern Hemisphere Glaciation (NHG) began at about 14 Ma (e.g., THIEDE et al. 1998). Glaciation of Antarctica, on the other hand, started much earlier, with large ice sheets first appearing near the Eocene/Oligocene boundary at about 34 Ma (e.g., LEAR et al. 2000, ZACHOS et al. 2008, ESCUTIA et al. 2011). With ACEX, however, the date of Northern Hemisphere cooling and the early onset of sea ice was pushed back into the Eocene (BACKMAN et al. 2006, 2008, MORAN et al. 2006, ST. JOHN 2008, STICKLEY et al. 2009). This early onset of Arctic sea-ice formation and the contemporaneous decrease in sea-surface temperatures are clearly reflected in the ACEX biomarker records (STEIN et al. 2014, 2015).

The first occurrence of sea-ice related diatoms, contempora-neously with IRD, was at about 47-46 Ma (when using the ACEX age model of BACKMAN et al. 2008; "Age Model 1") or 44-41 Ma (when using the alternate chronology of POIRIER & HILLAIRE-MARCEL 2011; "Age Model 2"; ages marked as Ma* in text below) (Fig. 10b and 10c). Iceberg transport was
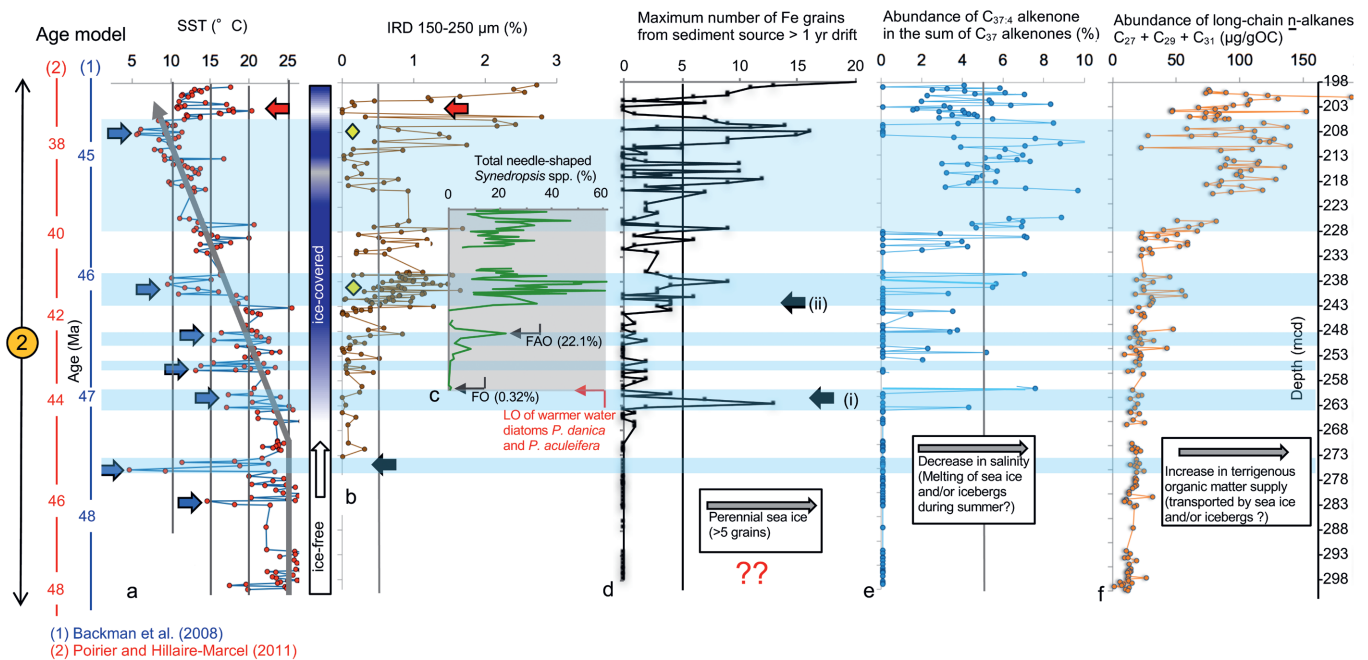

Fig. 10: (a): Alkenone-based sea-surface temperature (SST) (red circles; STEIN et al. 2014), **(b)**: abundance of ice-rafted debris (IRD) (brown circles, ST. JOHN 2008), **(c)**: abundance of sea-ice diatom species *Synedropsis* spp. (STICKLEY et al. 2009), **(d)**: maximum number of Fe grains from sediment sources with >1 yr drift time (assuming modern sea-ice drift rates) (DARBY 2014), **(e)**: abundances of $C_{37:4}$ alkenones (blue circles, STEIN et al. 2014), and **(f)**: long-chain n-alkanes indicative of higher-plant input (orange circles, STEIN et al. 2014), determined in the ACEX sequence from 298-198 meters below sea floor (mcd) (Interval 2 in Fig. 9). In the diatom record, the first occurrence (FO) and abundant occurrence (FAO) of the sea-ice species and the last occurrence (LO) of warmer water diatoms *Porotheca danica* and *Pterotheca aculeifera* are also shown. Large blue arrows indicate major cooling events; the large red arrow highlights a major warming event near 44.6 Ma. Large black arrows (i) and (ii) indicate major steps/increases in sea-ice cover. On the left-hand side, the two different age scales discussed in the text, are shown

Abb. 10: (a): Alkenon-basierende Oberflächenwassertemperaturen (SST) (rote Kreise; STEIN et al., 2014), **(b)**: Vorkommen von eistransportiertem Material (IRD) (braune Kreise; St. John, 2008), **(c)** Vorkommen der Meereis-Diatomee *Synedropsis* spp. (Stickley et al., 2009), **(d)**: Vorkommen von bestimmten eistransportierten Fe-Körnern (DARBY 2014), **(e)**: Konzentrationen von $C_{37:4}$ Alkenonen (blaue Kreise, STEIN et al. 2014), und **(f)**: langkettige n-Alkane als Anzeiger für höhere Landpflanzen (orange Kreise, STEIN et al. 2014), bestimmt in der ACEX-Abfolge zwischen 298-198 Kerntiefe (Interval 2 in Abb. 9). Große blaue Pfeile markieren Abkühlungsereignisse, der große rote Pfeil ein Erwärmungsereignis vor ca. 44.6 Ma. Große schwarze Pfeile (i) und (ii) markieren markante Zunahmen von Meereisverbreitung. Am linken Rand der Abbildung sind die beiden im Text diskutierten unterschiedlichen Altersmodelle angegeben.

probably also present in the middle Eocene, as indicated by mechanical surface-texture features on quartz grains from this interval (St. John 2008, Stickley et al. 2009). An early onset/intensification of NHGs during Eocene times is also supported by IRD records from the Greenland Basin ODP Site 913 (Eldrett et al. 2007, Tripati et al. 2008). These findings suggest that Earth's transition from the Greenhouse to the Icehouse world was probably bipolar, which points to greater control of global cooling linked to changes in greenhouse gases in contrast to tectonic forcing (Backman et al. 2006, 2008, Moran et al. 2006, DeConto et al. 2008, Stickley et al. 2009).

The cooling trend and onset of sea-ice formation recorded in the ACEX record, coinciding with the global post-Early Eocene Climate Optimum (EECO) cooling trend (Zachos et al. 2008), is also reflected in the ACEX sea-surface temperature (SST) (Fig. 10a; Stein et al. 2014). Prior to about 47 Ma (44 Ma* = "Age Model 2"), warm SSTs between 18 and 26 °C prevailed, interrupted by a prominent, short-lived cooling to 5-10 °C near 47.3 Ma (44.5 Ma*). At about 46.3 Ma (41.5

Ma*), summer SST dropped to <17 °C (range 8-17 °C), more or less coinciding with a significant increase in IRD (St. John 2008, Stickley et al. 2009), $C_{37:4}$ alkenones (Fig. 10e), and terrigenous organic matter (Fig. 10f). An absolute SST minimum of 6-8 °C was reached at about 44.8 Ma (37.8 Ma*), followed by a short but prominent warm phase with a SST around 17 °C near 44.6 Ma (37.5 Ma*). This warming event is characterized by the absence of IRD (Fig. 10b), interpreted to reflect lack of sea ice. Apart from this warm event, however, wide-spread sea ice seems to be the more typical phenomenon of the Arctic Ocean after about 45.5 Ma (40.5 Ma*) (Fig. 10).

Overall, the Arctic SST values remained surprisingly high, even in the upper part of the ACEX record where proxy data suggest the presence of sea ice. Hence, the alkenone SST probably represents rather the summer SST. Considering the strong seasonal temperature variability of >10 °C during the early-middle Eocene (Basinger et al. 1994, Greenwood & Wing 1995), on the other hand, favourable conditions for sea-ice formation must have occurred during winter-time (Stein et al. 2014).
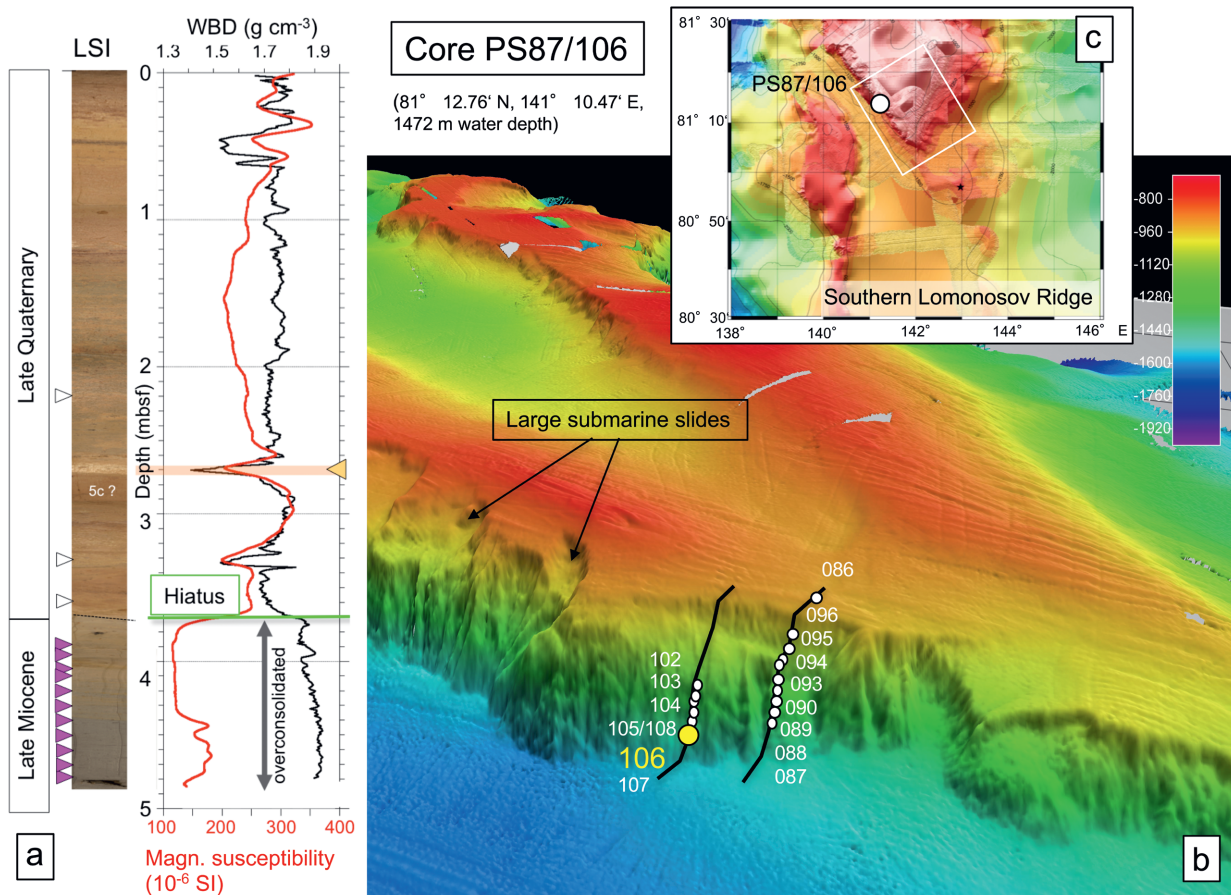

Fig. 11: (**a**): Line-scan image (LSI), wet-bulk density (WBD) and magnetic susceptibility records of Core PS87/106 (Stein et al. 2016). Purple and open triangles indicate presence or absence of alkenones, respectively. Green line marks depth of the hiatus. Below the hiatus, sediments are overconsolidated. (**b**): 3D image of the swath bathymetry of southern Lomonosov Ridge, showing major slide scars and escarpments, streamlined SE-NW oriented glacial lineations formed beneath grounded ice sheets/streams, and transects 1 and 2 with locations of sediment cores (Stein 2015, Stein et al. 2016). (**c**): Map of southern Lomonosov Ridge with location of Core PS87/106. White rectangle indicates area of the 3D image of Figure 11b.

Abb. 11: (**a**): Line-scan Aufnahme (LSI), Nassdichte (WBD) und magnetische Suszeptibilität in Kern PS87/106 (Stein et al. 2016). Violette und weiße Dreiecke zeigen das Vorhandensein bzw. die Abwesenheit von Alkenonen an. Die grüne Linie markiert den Hiatus zwischen den miozänen und quartären Sedimenten. Unterhalb des Hiatus sind die Sedimente überkonsolidiert. (**b**): Bathymetrische 3D-Darstellung vom Lomonosov-Rücken mit Abrisskanten großer untermeerischer Rutschungen, ausgedehnte SE-NW-orientierte Lineationen, die auf Erosion eines aufliegenden Eisschildes zurückzuführen sind, und Lokationen der auf den Transekten 1 und 2 genommenen Sedimentkerne (Stein 2015, Stein et al. 2016). (**c**): Bathymetrische Karte vom südlichen Lomonosov-Rücken mit Lokation des Kerns PS87/106. Das weiße Rechteck gibt das Gebiet der 3D-Aufnahme von Abbildung 11b wider.

Ice-free summers in the central Arctic Ocean during the Late Miocene

Late Miocene climatic conditions significantly warmer than today have been reconstructed from marine and terrestrial proxy records from different localities around the globe (ZACHOS et al. 2008, POUND et al. 2011, ZHANG et al. 2014). Quantitative SST proxy data from the High Arctic were restricted to a few terrestrial records (WOLFE 1994, UTE-SCHER et al. 2015). STEIN et al. (2016) complemented these studies with the first late Miocene SST and sea-ice records for the central Arctic Ocean, discussed in the following.

During "Polarstern" Expedition 87 in 2014, numerous submarine slide scars were discovered on both sides of the crest of Lomonosov Ridge over a distance of about 350 km between 81°07' N and 84°14' N in water depths from about 800 m to 1500 m (Fig. 11b; STEIN 2015, STEIN et al. 2016). Sediment removal from the steep slopes of the escarpments exposed older, normally deeply buried deposits at or near the present sea floor, allowing the retrieval of older sediments by gravity coring from "Polarstern". Sixteen sediment cores were recovered along two transects from water depths between 900 m and 1500 m (Fig. 11b; STEIN 2015). However, only Core PS87/106 recovered at the lower slope of Transect 2 (Fig. 11b), provides a clear indication that old sediments occur in the shallow sub-sea floor. In this core, a sharp unconformity (hiatus) occurs at 370 cm below sea floor (cmbsf) (Fig. 11a). This unconformity is characterized by a marked change in colour, an abrupt increase in wet-bulk density (related to enhanced sediment consolidation underneath the hiatus), a significant drop in magnetic susceptibility, and a major change in the biomarker composition. It separates this interval from the overlying unconsolidated upper Quaternary sediments (Fig. 11a; STEIN et al. 2016). The common occurrence of the acritarch *Decahedrella martinheadii* clearly indicates a late Miocene age for the lower part of the sedimentary sequence (STEIN et al. 2016; cf. MATTHIESSEN et al. 2009, SCHRECK et al. 2012). Reworking of these late Miocene palynomorphs is excluded based on the excellent preservation of the encountered delicate palynomorph specimens.

Using the lower 1.3 m thick section of Core PS87/106, STEIN et al. (2016) applied the IP_{25} sea-ice biomarker approach together with alkenone-based SST reconstructions (cf., Fig. 6) to investigate upper Miocene Arctic Ocean sea-ice and SST conditions. Within this study, these authors demonstrate for the first time that the late Miocene central Arctic Ocean was relatively warm with SSTs of about 5 °C and ice-free during summer, whereas sea ice occurred during spring and autumn/winter (Fig. 12b). That means, in contrast to the modern situation characterized by a perennial sea-ice cover and SST values <0 °C (Fig. 12a), a seasonal sea-ice coverage was predominent in the late Miocene.

Although at a first sight the short sedimentary section of Core PS87/106 only represents a short snapshot of late Miocene Arctic climate, more detailed information about the late Miocene climate on a regional to even global scale can be obtained from this record (STEIN et al. 2016). Based on the biomarker data, this late Miocene section of Core PS87/106 probably respresents almost one glacial/interglacial cycle with extended and reduced spring sea-ice conditions (Fig. 12b).

The (almost entire) absence of phytoplankton biomarkers and IP_{25} (PIP_{25} = "1") as well as low concentrations of terrigenous biomarkers may be explained by an extended to closed sea-ice cover and a very restricted spring season (Scenario 1 in Figs. 12b and 13a). Scenario 2, on the other hand, represents a transitional phase with a stable ice edge during an extended and productive spring season, characterized by maximum input of phytoplanktion biomarkers and IP_{25} (resulting in PIP_{25} values of 0.4-0.7) as well as maximum input of terrigenous biomarkers (and IRD) (Scenario 2 in Figs. 12b and 13b). The interval between scenarios 1 and 2 is characterized by very low to zero IP_{25} concentrations and increased concentrations of phytoplankton biomarkers, resulting in a distinct PIP_{25} minimum (Fig. 12b). This interval is interpreted as a period of minimum spring sea-ice extent (STEIN et al. 2016). Furthermore, maximum values of alkenones may reflect increased productivity of haptophyte algae during the summer season.

Using mean sedimentation rates of about 3.2 cm/ky as calculated independently from close-by gravity cores (STEIN et al. 2001), the duration of this cycle is about 40 ky, i.e., very similar to the 41 ky obliquity cycle (Fig. 12b). Hence, the record may represent just one obliquity cycle with ice-free conditions during summers in both the cold ("glacial") as well as the warm ("interglacial") phase of this climate cycle (Fig. 13a, 13b). As Core PS87/106 is of late Miocene age, ice-free summer conditions should have occurred in the central Arctic Ocean during the warmer Middle Miocene to early Late Miocene time interval a fortiori (STEIN et al. 2016).

Middle Eocene and late Miocene Arctic Ocean sea-ice coverage: Perennial versus seasonal

In contrast to the biomarker-based reconstructions described above, an Arctic Ocean perennial sea-ice cover from middle Miocene onwards has been proposed by DARBY (2008) and KRYLOV et al. (2008) based on provenance studies of ice-rafted debris (IRD) in ACEX sediments. More recently, DARBY (2014) postulated ephemeral formation of even perennial sea ice in the Arctic Ocean during the middle Eocene. Darby's statement is based on the occurrence of specific coarse Fe grains (IRD) indicative of a distal source area (such as North America or Siberia). Taking the IRD with a North American or East Siberian origin found in the ACEX sediments and using modern sea-ice drift trajectories and velocities, these authors concluded that more than one year was needed to transport the sediments entrained in sea ice to the ACEX location. Hence, sea ice must have survived the summer melting season to reach the ACEX Site.

The onset of deposition of such Fe grains at the ACEX site (Fig. 10d) is almost contemperaneous with the drop in SST (Fig. 10a) as well as the appearance of IRD (Fig. 10b), sea-ice diatoms (Fig. 10c) and $C_{37:4}$ alkenones (Fig. 10e). The latter data as well as the occurrence of dinoflagellates and agglutinated benthic foraminifers (CRONIN et al. 2008, MATTHIESSEN et al. 2009), however, are more indicative of a seasonal sea-ice cover (STEIN et al. 2014, 2015). Thus, if present, phases of perennial sea ice should have been more the exception in the middle Eocene whereas seasonal sea ice should have been the rule. Also for the late Miocene time interval, biomarker data point to a predominantly seasonal sea-ice cover in the central Arctic Ocean as discussed above (Figs. 12 and 13; STEIN et al. 2016).

Based on a simulation of ice-drift pattern and velocities under permanent and seasonal ice conditions, TREMBLAY et al. (2015) have recently demonstrated that sea-ice drift was probably significantly faster under warmer climatic conditions with less or much thinner sea ice than today. They conclude that the presence of ice-rafted sediment of Eurasian and North American origin at the North Pole is not a definite indication of a perennial sea-ice cover in the Arctic Ocean. This may imply that the main assumption of DARBY (2008, 2014) and KRYLOV et al. (2008) should be regarded critically.

CONCLUSIONS AND OUTLOOK

The Arctic paleoceanographic and paleoclimate results from ACEX were unprecedented and – in combination with additional spotty information from a few short sediment cores – give important insight into the long-term Arctic sea-ice history. Here, especially the early onset of seasonal sea ice in the central Arctic Ocean during the middle Eocene and the presence of ice-free conditions during summers throughout the middle-late Miocene have to be highlighted. However, major questions related to the climate history development of the Arctic Ocean from Greenhouse to Icehouse conditions during early Cenozoic times remain unanswered, largely due to the major mid-Cenozoic hiatus and partly to the poor recovery of the ACEX record (Figs. 5 and 9a). In order to decipher the pre-Quaternary climate (and sea-ice) history of this unique and sensitive, but still not well known region on Earth in more detail, long continuous sedimentary records to be obtained only by scientific drilling, are needed. These records are planned to be recovered within a new IODP drilling campaign on the southern Lomonosov Ridge (IODP Expedition 377, ARCOP 2017). Based on new PS87 seismic data (STEIN et al. 2015), about 200 m of Plio-Pleistocene, >600 m of Miocene, and >300 m of Oligocene-Eocene may be reco-
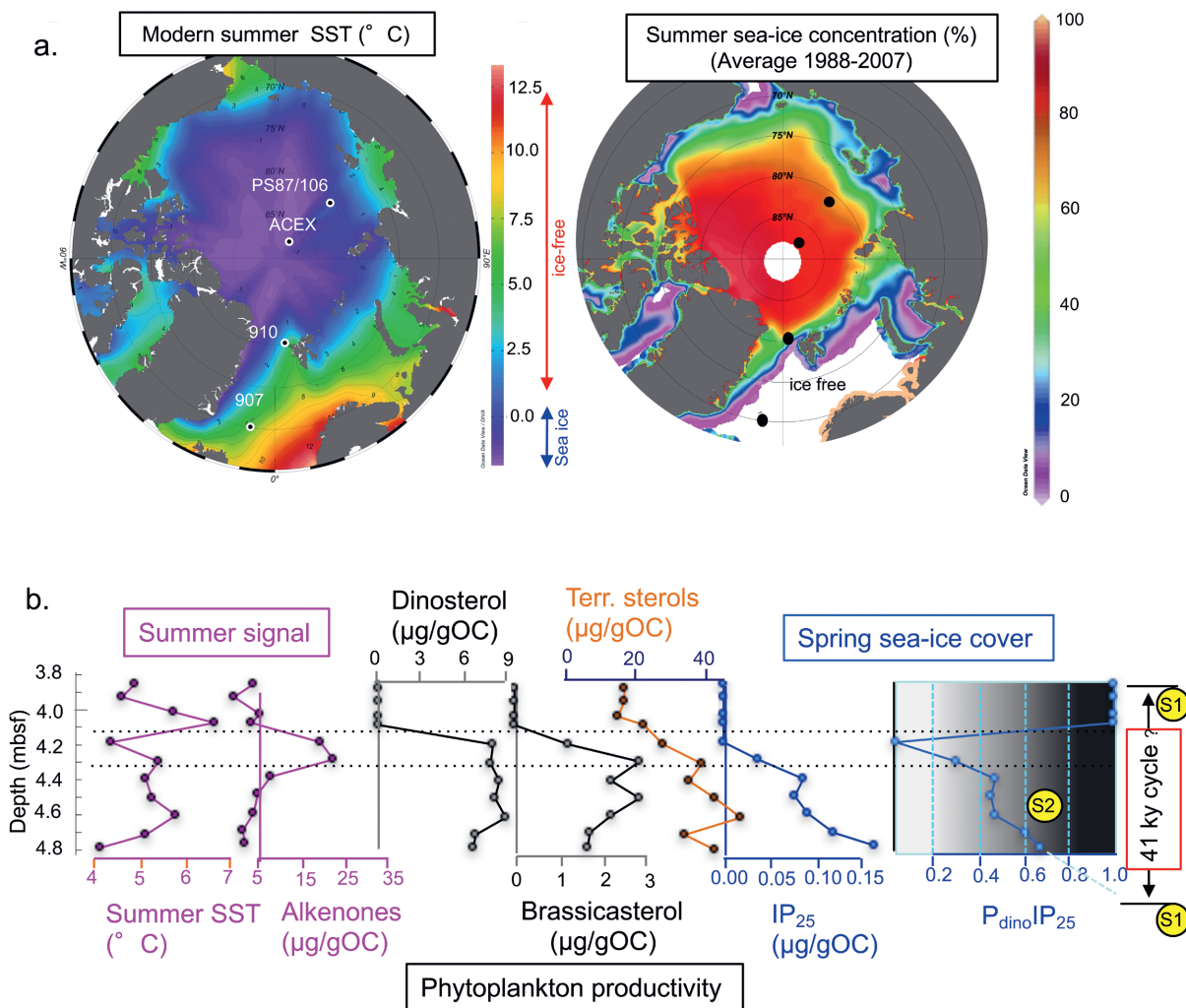

Fig. 12: (**a**): Maps of modern August sea-surface temperature (SST) and summer sea-ice concentration with locations of the ACEX Site and Core PS87/106. SST data (average of 1955 to 2012) from WORLD OCEAN ATLAS (2013); sea-ice data (average of 1988 to 2007) from NCSID. Maps produced with OCEAN DATA VIEW software (source: http://odv.awi.de/). (**b**): Proxy evidence from Core PS87/106 for late Miocene Arctic Ocean climate conditions (from STEIN et al. 2016): alkenone-based sea-surface temperature (SST), concentrations of alkenones, dinosterol and brassicasterol as proxy for primary productivity, concentrations of terrigenous sterols (sum of campesterol and ß-sitosterol), concentrations of sea-ice proxy IP_{25}, and sea-ice index $P_{dino}IP_{25}$ (for background and calculation see STEIN et al. 2016).

Abb. 12: (**a**): Karten der heutigen August-Oberflächenwassertemperatur (SST) und Sommer-Meereisverbreitung mit Lokationen von ACEX-Site und Kern PS87/106. SST-Daten (Mittelwerte 1955 bis 2012) aus WORLD OCEAN ATLAS (2013). Meereisdaten (Mittelwerte von 1988 bis 2007) aus NISDC (2013). Die Abbildungen sind mit dem Programm „Ocean Data View" (Quelle: http://odv.awi.de/) erstellt worden. (**b**): Rekonstruktionen der spätmiozänen Klimabedingungen nach Proxy-Daten von Kern PS87/106 (aus STEIN et al. 2016).

vered at the proposed drill sites (Fig. 14). From the total of ten potential drill sites those from the southern Lomonosov Ridge have been identified as "first-priority sites", as from this area detailed seismic data but also comprehensive information from numerous sediment cores recovered during "Polarstern" expeditions in 1995, 2008 and 2014 are available (Fig. 15; STEIN (2015) and further references therein). The outcome of such a new program will certainly help to improve our understanding of the complex ocean-atmosphere-ice system in the polar high northern latitudes and its role in the past, modern and future global climate.
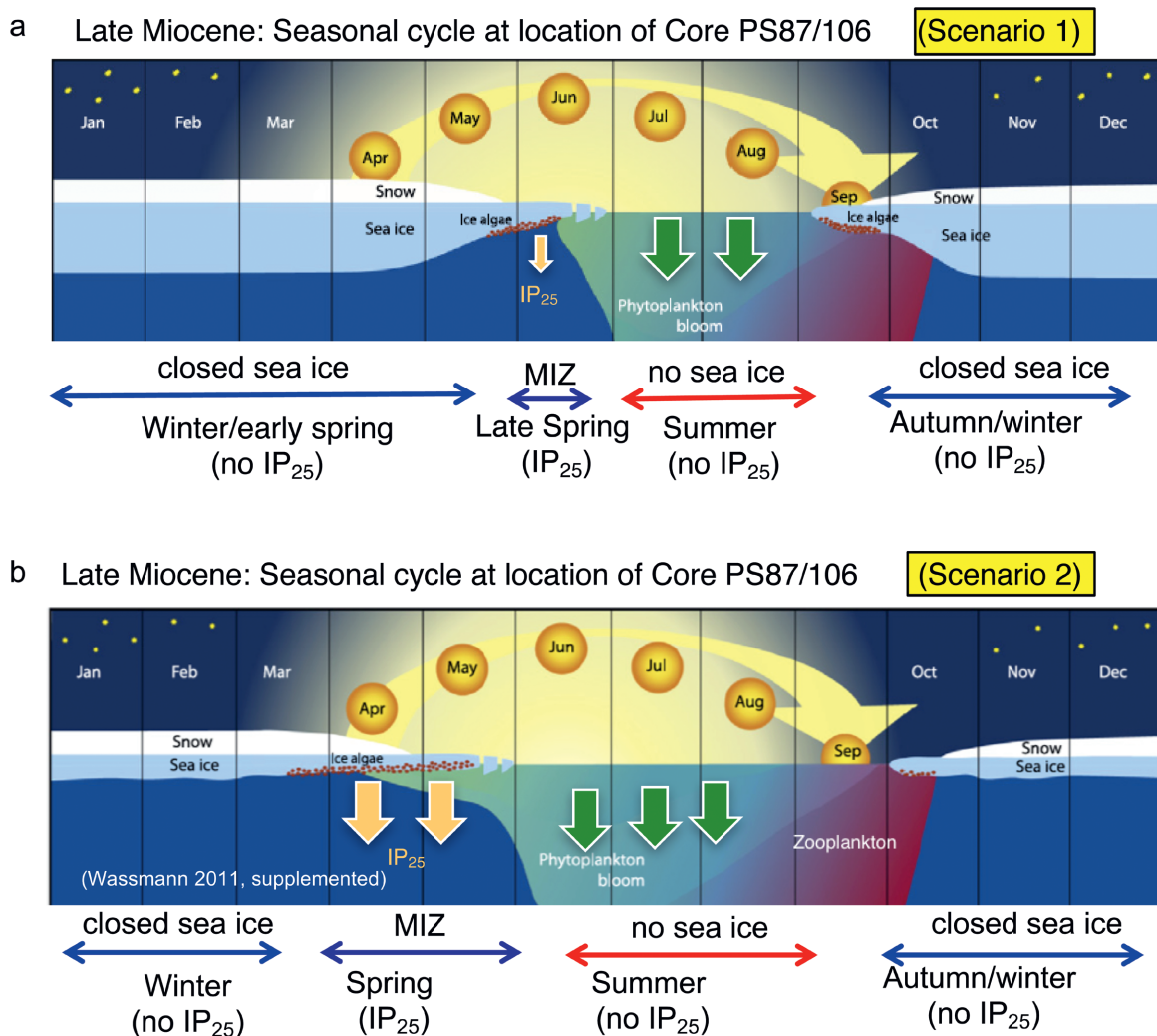
Fig. 13: The seasonal sea-ice cycle and related principal processes controlling productivity and carbon flux in the central Arctic Ocean during the late Miocene are shown for two different scenarios (STEIN et al. 2016). **(a):** Scenario 1 ("cold situation"): restricted period of late spring sea-ice algae productivity and very reduced fluxes (almost to zero) of IP$_{25}$ and spring phytoplankton biomarkers. **(b):** Scenario 2 ("warmer/transitional situation") with extended period of spring sea-ice algae productivity as well as increased IP$_{25}$ and phytoplankton biomarker fluxes. MIZ: Marginal Ice Zone, i.e., ice-edge situation. The dark period, height of the sun and changing thickness of snow and ice over the year as well as phytoplankton, zooplankton, and sea-ice productivity are shown. IP$_{25}$ values for the different seasons are indicated (after WASSMANN 2011, supplemented).

Abb. 13: Schematische Darstellung des jährlichen Meereiszyklus und der wichtigsten Steuerungsprozesse von Produktion und Fluss von Phytoplankton, Zooplankton und Eisalgen im zentralen spätmiozänen Arktischen Ozean für zwei unterschiedliche Szenarien: **(a)** Szenario 1: „Kaltphase"; **(b)** Szenario 2: „wärmere Übergangsphase" (STEIN et al. 2016, ergänzt). MIZ: Eisrandzone und IP$_{25}$-Vorkommen während der unterschiedlichen Jahreszeiten sind angegeben. Die schematische Darstellung basiert auf WASSMANN (2011, ergänzt).
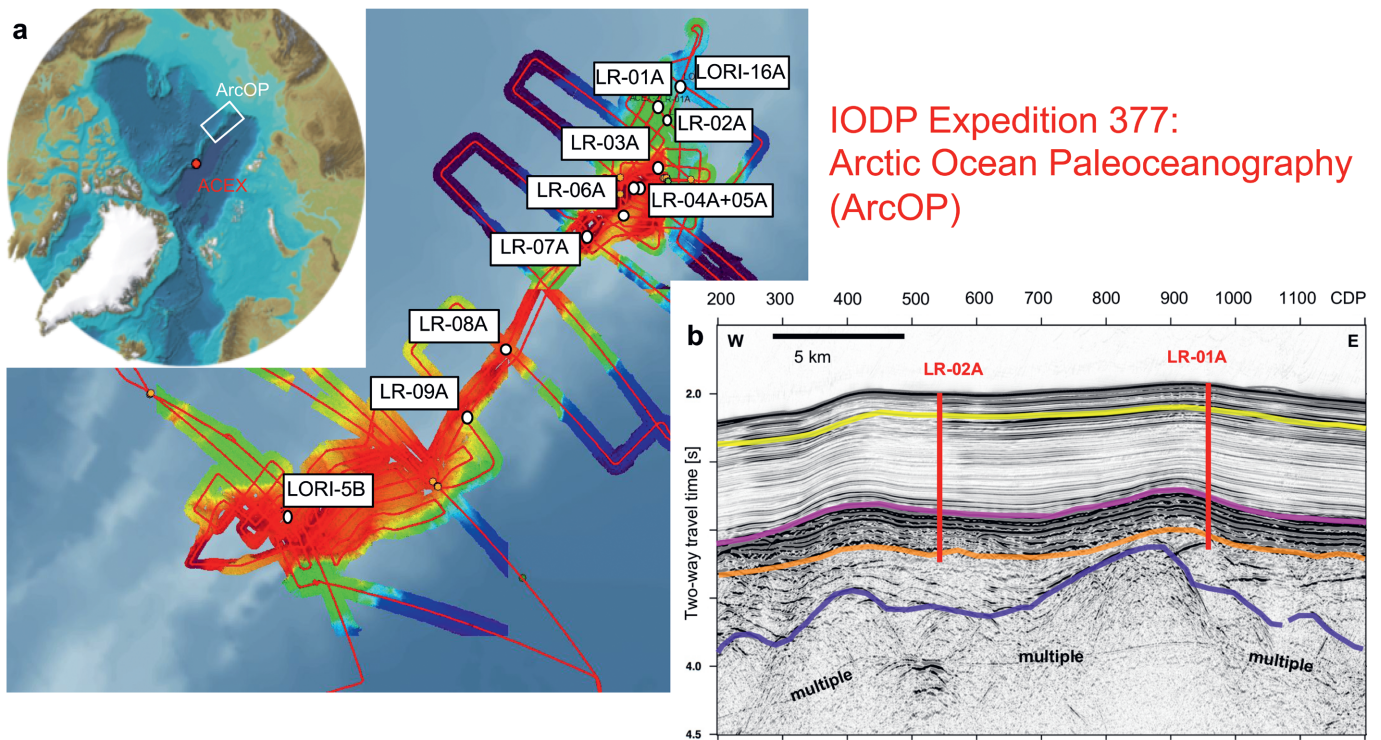
Fig. 14: Track lines of multibeam (Hydrosweep) bathymetric and Parasound echosounding survey carried out during "Polarstern" Expedition PS87 (Stein 2015) with locations of proposed IODP drill sites for IODP Expedition 377 (ArcOP 2017, Stein et al. 2015); small map in **(a):** International Bathymetric Chart of the Arctic Ocean (IBCAO, Jakobsson et al. 2012) with location of the ACEX drill site and the area of PS87 site survey/work area of planned IODP Expedition 377. **(b):** Seismic profile of line AWI-20140307 with interpretation of seismic reflectors: Top of Miocene: "yellow reflector", top of Oligocene: "pink reflector") corresponding to top of the HARS ("high-amplitude reflector sequence"), and lower Eocene: "orange reflector" (Stein et al. 2015). Location and stratigraphic range of proposed drill sites are shown at LR-01A and LR-02A.

Abb. 14: Karte der während Expedition PS87 mit "Polarstern" durchgeführten bathymetrischen und sedimentechographischen Vermessungen (Stein 2015) mit den für die IODP-Expedition 377 (ArcOP 2017) vorgeschlagenen Bohrlokationen (Stein et al. 2015; **(a):** Übersicht auf kleiner Karte (International Bathymetric Chart of the Arctic Ocean -IBCAO- Jakobsson et al. 2012) mit Lokation der ACEX-Bohrung und Lage des Arbeitsgebiets der Expedition PS87 bzw. der geplanten IODP-Expedition 377. **(b):** Seismisches Profil AWI-20140307 mit Interpretation der Hauptreflektoren: Top Miozän ("gelber Reflektor"), Top Oligozän: "rötlicher Reflektor") und unteres Eozän: "oranger Reflektor" mit Lokationen und stratigraphischer Reichsweite der vorgeschlagenen Bohrpunkte LR-01A und LR-02A (Stein et al. 2015).
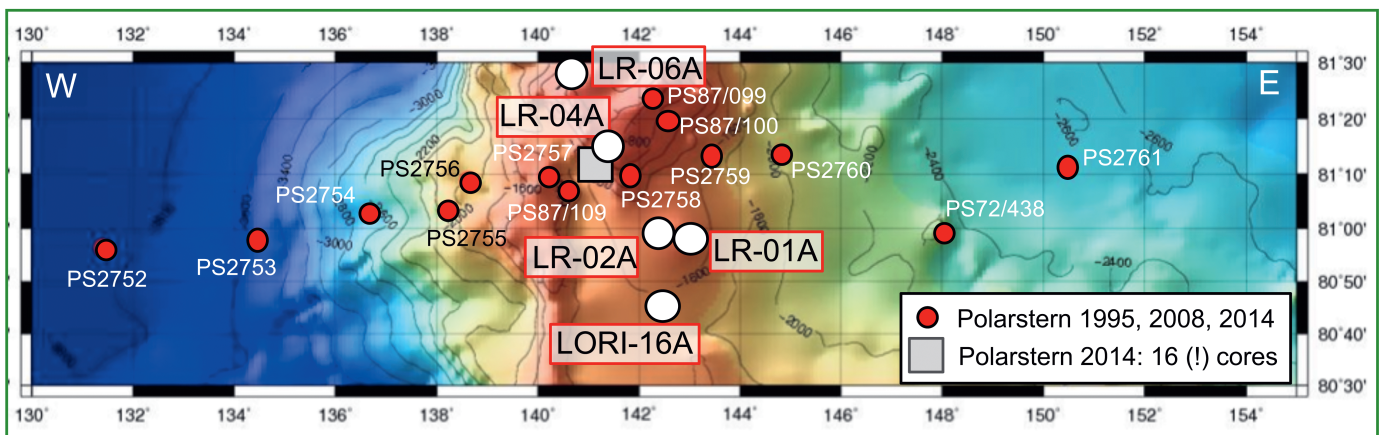

Fig. 15: West (W) – East (E) transect across the Lomonosov Ridge near to the Siberian margin showing locations of the "first-priority" ArcOP drill sites LR-01A, LR02A, LR-04A, LR-04A, and LORI-16A (large white circles) as well as the locations of numerous sediment cores recovered during "Polarstern" expeditions in 1995, 2008, and 2014 (red circles and blue box) (for further details and references see Stein 2015).

Abb. 15: West – Ost-Schnitt über den südlichen Lomonosov-Rücken mit „first-priority" ArcOP-Bohrlokationen LR-01A, LR02A, LR-04A, LR-04A und LORI-16A sowie Lokationen von zahlreichen Sedimentkernen, die auf „Polarstern"-Expeditionen in den Jahren 1995, 2008 und 2014 gewonnen wurden (weitere Details in Stein 2015).

References / Online

ArcOP (2017) Expedition 377 Arctic Ocean Paleoceanography (accessed 28 July 2017) <http://www.ecord.org/expedition377/>

NISDC National Ice and Snow data center (2013) <http//nsidc.org/> (accessed 25 Aug. 2017).

Aagaard, K. & Carmack, E.C. (1989): The role of sea ice and other fresh water in the Arctic circulation.- J. Geophys. Res. 94(C10): 14485-14498.

Backman, J., Jakobsson, M., Frank, M., Sangiorgi, F., Brinkhuis, H., Stickley, C., O'Regan, M., Løvlie, R., Pälike, H., Spofforth, D., Gattacecca, J., Moran, K., King, J. & Heil, C. (2008): Age model and core-seismic integration for the Cenozoic Arctic Coring expedition sediments from the Lomonosov Ridge.- Paleoceanography 23, doi: 10.1029/2007PA001476.

Backman, J., Moran, K., McInroy, D.B., et al. (2006): Proceedings IODP, 302, College Station, Texas (Integrated Ocean Drilling Program Management International, Inc.).- doi:10.2204/iodp.proc.302.104.2006.

Bard, E., Rostek, F., Turon, J.-L. & Gendreau, S. (2000): Hydrological impact of Heinrich events in the subtropical northeast Atlantic.- Science 289: 1321-1324.

Basinger, J.F., Greenwood, D.G. & Sweda, T. (1994): Early Tertiary vegetation of Arctic Canada and its relevance to paleoclimatic interpretation.- In: M.C. BOULTER & H.C. FISCHER (eds): Cenozoic Plants and Climates of the High Arctic, NATO ASI Ser., Ser. 1, 127: 175-198.

Belt, S.T., Massé, G., Rowland, S.J. et al. (2007): A novel chemical fossil of palaeo sea ice: IP$_{25}$.- Organic Geochemistry 38: 16-27.

Belt, S.T., Cabedo-Sanz, P., Smik, L., Navarro-Rodriguez, A., Berben S.M.P., Knies, J. & Husum, K. (2015): Identification of paleo Arctic winter sea ice limits and the marginal ice zone: Optimised biomarker-based reconstructions of late Quaternary Arctic sea ice.- Earth Planet. Sci. Lett. 431: 127-139.

Belt, S.T. & Müller, J. (2013): The Arctic sea ice biomarker IP$_{25}$: a review of current understanding, recommendations for future research and applications in palaeo sea ice reconstructions.- Quat. Sci. Rev. 79: 9-25.

Brown, T.A., Belt, S.T., Tatarek, A. & Mundy, C.J. (2014): Source identification of the Arctic sea ice proxy IP$_{25}$.- Nature Communicat. 5: 4197.

Brassell, S.C., Eglinton, G., Marlowe, I.T., Pflaumann, U.] Sarntheim, M. (1986): Molecular stratigraphy: a new tool for climate assessment. Nature 320: 129-133.

Broecker, W.S. (1997): Thermohaline Circulation, the Achilles Heel of Our Climate System: Will Man-Made CO$_2$ Upset the Current Balance? Science 278: 1582-1588.

Cavalieri, D.J. & Parkinson, C.L. (2012): Arctic sea ice variability and trends, 1979-2010.- The Cryosphere 6: 881-889.

Clark, D.L., Byers, C.W. & Pratt, L.M. (1986): Cretaceous black mud from the central Arctic Ocean.- Paleoceanography 1: 265-271.

Clark, P.U., Pisias, N.G., Stocker, T.F. & Weaver, A.J. (2002): The role of the thermohaline circulation in abrupt climate change.- Nature 415: 863-869.

Conte, M.H., Eglinton, G. & Madureira, L.A.S. (1992): Long-chain alkenones and alkyl alkenoates as palaeotemperature indicators: their production, flux and early sedimentary diagenesis in the eastern North *Atlantic*.- Org. Geochem. 19: 287-298.

Cronin, T.M., Smith, S.A., Eynaud, F., O'Regan, M. & King, J. (2008): Quaternary paleoceanography of the central Arctic based on Integrated Ocean Drilling Program Arctic Coring Expedition 302 foraminiferal assemblages.- Paleoceanography 23: (doi:10.1029/2007PA001484).

Cronin, T.M., Polyak, L., Reed, D., Kandiano, E.S., Marzen, R.E. & Council, E.A. (2013): A 600-ka Arctic sea-ice record from Mendeleev Ridge based on ostracodes.- Quat. Sci. Rev. 79: 157-167

Darby, D.A. (2008): The Arctic perennial ice cover over the last 14 million years.- Paleoceanography 23, doi:10.1029/2007PA001479.

Darby, D.A. (2014): Ephemeral formation of perennial sea ice in the Arctic Ocean during the middle Eocene.- Nature Geoscience 7:210-213, doi: 10.1038/NGEO2068.

Davies, A., Kemp, A.E.S. & Pälike, H. (2011): Tropical ocean-atmosphere controls on inter-annual climate variability in the Cretaceous Arctic.- Geophys. Res. Lett. 38: doi: 10.1029/2010GL046151

Davies, A., Kemp, A.E.S. & Pike, J. (2009): Late Cretaceous seasonal ocean variability from the Arctic.- Nature 460: 254-258.

DeConto, R.M., Pollard, D., Wilson, P.A., Pälike, H., Lear, C.H. & Pagani, M. (2008): Thresholds for Cenozoic bipolar glaciations.- Nature 455: 652-656.

Dell'Agnese, D.J. & Clark, D.L. (1994): Siliceous microfossils from the warm Late Cretaceous and Early Cenozoic Arctic Ocean.- J. Paleont. 68: 31-47.

De Vernal, A., Gersonde, R., Goose, H., Seidenkrantz, M.-S. & Wolff, E.W. (2013): Sea ice in the paleoclimate system: the challenge of reconstructing sea ice from proxies - an introduction.- Quat. Sci. Rev. 79: 1-8.

Eldrett, J.S., Harding, I.C., Wilson, P.A., Butler, E. & Roberts, A.P. (2007): Continental ice in Greenland during the Eocene and Oligocene.- Nature 446: 176-179, doi:10.1038/nature05591.

Escutia, C., Brinkhuis, H., Klaus, A. & the IODP Expedition 318 Scientists (2011): IODP Expedition 318: from Greenhouse to Icehouse at the Wilkes Land Antarctic margin.- *Scientific Drilinng* 12: 15-23.

Firth, J.V. & Clark, D.L. (1998): An early Maastrichtian organic-walled phytoplankton cyst assemblage from an organic-walled black mud in Core F1-533, Alpha Ridge: evidence for upwelling conditions in the Cretaceous Arctic Ocean.- Mar. Micropaleont. 34: 1-27.

Flato, G.M. & Participating CMIP Modelling Groups (2004): Sea ice and its response to CO$_2$ forcing as simulated by global climate models.- Clim. Dynamics 23: 229-241.

Friedrich, O., Norris, R.D. & Erbacher, J. (2012): Evolution of middle to late Cretaceous oceans – a 55 m.y. record of Earth's temperature and carbon cycle.- Geology 40: 107-110.

Greenwood, D.G. & Wing, S.L. (1995): Eocene continental climates and latitudial temperatures gradients.- Geology 23: 1044-1048.

Ho, S.L., Mollenhauer, G., Fietz, S., Martinez-Garcia, A., Lamy, F., Rueda, G., Schipper, K., Méheust, M., Rosell-Melé, A., Stein, R. & Tiedemann, R. (2014): Appraisal of the TEX$_{86}$ and TEX$_{86}^L$ thermometries in the subpolar and polar regions. Geochim. Cosmochim. Acta 131: 213-226, doi: 10.1016/j.gca.2014.01.001.

Huguet, C., Schimmelmann, A., Thunell, R., Lourens, L.J., Sinninghe Damsté, J.S. & Schouten, S. (2007): A study of TEX 86 paleothermometer in the water column and sediments of the Santa Barbara Basin, California.- Paleoceanography 22: PA3203, doi:1029/2006PA001310

Jackson, H.R., Mudie, P.J. & Blasco, S.M. (1985): Initial geological report on CESAR – The Canadian Expedition to study the Alpha Ridge, Arctic Ocean.- Geol. Surv. Can. Pap. 84-22: 1-177.

Jakobsson M., Backman, J., Rudels, B., Nycander, J., Frank, M., Mayer, L., Jokat, W., Sangiorgi, F., O'Regan, M., Brinkhuis, H., King, J. & Moran, K. (2007): The early Miocene onset of a ventilated circulation regime in the Arctic Ocean.- Nature 447: 986-990.

Jenkyns, H.C., Forster, A., Schouten, S. & Sinninghe Damsté, J.S. (2004): High temperatures in the late Cretaceous Arctic Ocean.- Nature 432: 888-892.

Jakobsson, M., Mayer, L., Coakley, B., Dowdeswell, J.A., Forbes, S., Fridman, B., Hodnesdal, H., Noormets, R., Pedersen, R., Rebesco, M., Schenke, H.W., Zarayskaya, Yu., Accettella, D., Armstrong, A., Anderson, R.M., Bienhoff, P., Camerlenghi, A., Church, I., Edwards, M., Gardner, J.V., Hall, J.K., Hell, B., Hestvik, O., Kristoffersen, Y., Marcussen, C., Mohammad, R., Mosher, D., Nghiem, S.V., Pedrosa, M.T., Travaglini, P.G., and Weatherall, P. (2012): The International Bathymetric Chart of the Arctic Ocean (IBCAO) Version 3.0.- Geophys. Res. Lett. 39(12): L12609.

Kitchell, J.A. & Clark, D.L. (1982): Late Cretaceous-Paleogene paleogeography and paleocirculation: evidence of north polar upwelling.- Palaeogeogr. Palaeoclimatol. Palaeoecol. 40: 135-165.

Knies, J., Müller, C., Nowaczyk, N., Vogt, C. & Stein, R. (2000): A multiproxy approach to reconstruct the environmental changes along the Eurasian continental margin over the last 150 kyr.- Mar. Geol. 163: 317-344.

Koç, N., Jansen, E. & Haflidason, H. (1993.): Paleoceanographic reconstructions of surface ocean conditions in the Greenland, Iceland and Norwegian seas through the last 14 ka based on diatoms.- Quat. Sci. Rev. 12: 115-140.

Krylov, A.A., Andreeva, I.A., Vogt, C., Backman, J., Krupskaya, V.V., Grikurov, G.E., Moran, K. & Shoji, H. (2008): A Shift in Heavy and Clay Mineral Provenance Indicates a Middle Miocene Onset of a Perennial Sea-Ice Cover in the Arctic Ocean.- Paleoceanography 23: PA1S06, doi: 10.1029/2007PA001497.

Lear, C.H., Elderfield, P.A. & Wilson, P.A. (2000): Cenozoic deep-sea temperatures and global ice volumes from Mg/Ca in benthic foraminiferal calcite.- Sci. 287: 269-272.

Macdonald, R.W., Sakshaug, E. & Stein, R. (2004): The Arctic Ocean: Modern Status and Recent Climate Change.- In: R. STEIN, R. & R,W, MACDONALD, R.W. (eds.), The Organic Carbon Cycle in the Arctic Ocean, Springer Verlag, Heidelberg,. 6-21.

Marlowe, I.T., Brassell, S.C., Eglinton, G. & Green, J.C. (198): Long chain unsaturated ketones and esters in living algae and marine sediments. Org. Geochem. 6:135-141.

Marlowe, I.T., Brassell, S.C., Eglinton, G. & Green, J.C. (1990): Long-chain alkenones and alkyl alkenoates and the fossil coccolith record of marine sediments.- Chem. Geol. 88: 349-375.

Matthiessen, J., Knies, J., Nowaczyk, N.R. & Stein, R. (2001): Late Quaternary dinoflagellate cyst stratigraphy at the Eurasian continental margin, Arctic Ocean: indications for Atlantic water inflow in the past 150,000 years.- Glob. Planet. Change 31: 65-86

Matthiessen, J., Brinkhuis, H., Poulsen, N. & Smelror, M. (2009): *Decahedrella martinheadii* Manum 1997 – a stratigraphically and paleoenvironmentally useful Miocene acritarch of the mhigh northern latitudes.- Micropaleontology 55: 171-186.

Miller, K.G., Fairbanks, R.G. & Mountain, G.S. (1987): Tertiary oxygen isotope synthesis, sea level history, and continental margin erosion.- Paleoceanography 2: 1-19.

Moran, K., Backman, J., Brinkhuis, H., Clemens, S.C., Cronin, T., Dickens, G.R., Eynaud, F., Gattacceca, J., Jakobsson, M., Jordan, R.W., Kaminski, M., King, J., Koc, N., Krylov, A., Martinez, N., Matthiessen, J., McInroy, D., Moore, T.C., Onodera, J., O'Regan, A.M., Pälike, H., Rea, B., Rio, D., Sakamoto, T., Smith, D.C., Stein, R., St. John, K., Suto, I., Suzuki, N., Takahashi, K., Watanabe, M., Yamamoto, M., Frank, M., Jokat, W. & Kristoffersen, Y. (2006): The Cenozoic palaeoenvironment of the Arctic Ocean.- Nature 441: 601-605.

Müller, P.J., Kirst, G., Ruhland, G., von Storch, I. & Rosell-Melé, A. (1998): Calibration of the alkenone paleotemperature index U^k_{37}-based on core-tops from the eastern South Atlantic and the global ocean (60 degrees N - 60 degrees S).- Geochim. Cosmochim. Acta 62(10): 1757-1772.

Müller J., Massé G., Stein R. & Belt S.T. (2009): Variability of sea-ice conditions in the Fram Strait over the past 30,000 years.- Nature Geosci. 2: 772–776.

Müller, J., Wagner, A., Fahl, K., Stein, R., Prange, M. & Lohmann, G. (2011): Towards quantitative sea-ice reconstructions in the northern North Atlantic: A combined biomarker and numerical modeling approach.- Earth Planet. Sci. Lett. 306: 137-148

Nørgaard-Pedersen, N., Spielhagen, R.F., Erlenkeuser, H., Grootes, P.M., Heinemeier, J. & Knies, J. (2003): The Arctic Ocean during the Last Glacial Maximum: atlantic and polar domains of surface water mass distribution and ice cover. -Paleoceanography 18: 1-19.

PALAEOSENS Project-Members (2012): Making sense of palaeoclimate sensitivity.- Nature 491: 683-691, doi: 10.1038/nature11574.

Peng, G., Meier, W.N., Scott, D.J. & Savoie, M.H. (2013): A long-term and reproducible passive microwave sea ice concentration data record for climate studies and monitoring.- Earth Syst. Sci. Data 5: 311-318.

Pflaumann, U., Sarnthein, M., Chapman, M., d'Abreu, L., Funnell, B., Huels, M., Kiefer, T., Maslin, M., Schulz, H., Swallow, J., van Krefeld, S., Vautravers, M., Vogelsang, E. & Weinelt, M. (2003): Glacial North Atlantic: sea-surface conditions reconstructed by GLAMAP 2000.- Paleoceanography 18(3): 1065, doi:10.1029/2002 PA000774.

Poirier, A. & Hillaire-Marcel, C. (2011): Improved Os-isotope stratigraphy of the Arctic Ocean.- Geophys. Res. Lett. 38: L14607, doi: 10.1029/2011GL047953.

Polyak, L., Alley, R.B., Andrews, J.T., Brigham-Grette, J., Cronin, T.M., Darby, D.A., Dyke, A.S., Fitzpatrick, J.J., Funder, S., Holland, M., Jennings, A.E., Miller, G.H., O'Regan, M., Savelle, J., Serreze, M., St. John, K., White, J.W.C. & Wolff, E. (2010): History of sea ice in the Arctic.- Quat. Sci. Rev. 29(15-16): 1757-1778.

Pound, M.J., Haywood, A.M., Salzmann, U., Riding, J.B., Lunt, D.J. & Hunter, S.J. (2011): A Tortonian (Late Miocene, 11.61-7.25 Ma) global vegetation reconstruction. Palaeogeogr. Palaeoclimatol. Palaeoecol. 300: 29-45.

Prahl, F.G. & Wakeham, S.G. (1987): Calibration of unsaturation pattern in long-chain ketone compositions for paleotemperature assessment.- Nature 330: 367-369.

Rosell-Melé, A. (1998): Interhemispheric appraisal of the value of alkenone indices as temperature and salinity proxies in high-latitude locations.- Paleoceanography 13(6): 694-703.

Rosell-Melé, A., Jansen, E. & Weinelt, M. (2002): Appraisal of a molecular approach to infer variations in surface ocean freshwater inputs into the North Atlantic during the last glacial.- Global Planet. Change 34(3-4): 143-152.

Sakshaug, E. (2004): Primary and Secondary Production in the Arctic Seas.- In: R. STEIN & R.W. MACDONALD (eds), The Organic Carbon Cycle in the Arctic Ocean. Springer Verlag, Heidelberg, 57-82.

Schouten, J., Hopmans, E.C. & Sinninghe Damsté, J.S. (2004): The effect of maturity and depositional redox conditions on archaeal tetraether lipid palaeothermometry.- Org. Geochem. 35: 567-571.

Schouten, S., Hopmans, E.C., Schefuss, E. & Sinninghe Damsté, J.S. (2002): Distributional variations in marine crenarchaeotal membrane lipids: A new tool for reconstructing ancient sea water temperatures?.- Earth Planet. Sci. Lett. 204: 265-274.

Schreck, M., Matthiessen, J. & Head, M.J. (2012): A magnetostratigraphic calibration of Middle Miocene through Pliocene dinoflagellate cyst and acritarch events in the Iceland Sea (Ocean Drilling Program Hole 907A).- Rev. Palaeobot. Palynol. 187: 66-94.

Serreze, M.C. & Barry, R.G. (2011): Processes and impacts of Arctic amplification: A research synthesis.- Global Planet. Change 77: 85-96.

Serreze, M.C., Holland, M.M. & Stroeve, J. (2007): Perspectives on the Arctic's shrinking sea-ice cover.- Science 315: 1533-1536.

Sicre, M.A., Bard, E., Ezat, U. & Rostek, F. (2002) Alkenone distributions in the North Atlantic and Nordic sea surface waters.- Geochem. Geophys. Geosyst. 3(2): 1013, doi: 10.1029/2001GC000159.

Smik, L., Cabedo-Sanz & Belt, S.T. (2016): Semi-quantitative estimates of paleo Arctic sea-ice concentration based on source-specific highly branched isoprenoid alkenes: A further development of the PIP25 index.- Org. Geochem. 92: 63-69.

Spielhagen, R.F., Baumann, K.-H., Erlenkeuser, H., Nowaczyk, N.R.,

Nørgaard-Pedersen, N., Vogt, C. & Weiel, D. (2004): Arctic Ocean deep-sea record of Northern Eurasian ice sheet history.- Quat. Sci. Rev. 23 (11-13): 1455-1483.

Stein, R. (ed.) (2015): The Expedition PS87 of the Research Vessel Polarstern to the Arctic Ocean in 2014.- Rep. Polar Mar. Res. 688: 1-273, <http://epic.awi.de/37728/1/BzPM_0688_2015.pdf>.

Stein, R. (2007): Upper Cretaceous/Lower Tertiary black shales near the North Pole: Organic-carbon origin and source-rock potential.- Mar. Petrol. Geol. 24: 67-73.

Stein, R. (2008): Arctic Ocean Sediments: Processes, Proxies, and Palaeoenvironment.- Developments Marine Geology Vol. 2: 1-587 Elsevier, Amsterdam.

Stein, R., Boucsein, B., Fahl, K., Garcia de Oteyza, T., Knies, J. & Niessen, F. (2001): Accumulation of particulate organic carbon at the Eurasian continental margin during late Quaternary times: Controlling mechanisms and paleoenvironmental significance.- Global Planett Change 31/1-4: 87-102.

Stein, R., Boucsein, B. & Meyer, H. (2006): Anoxia and high primary production in the Paleogene central Arctic Ocean: First detailed records from Lomonosov Ridge.- Geophys. Res. Lett. 33: L18606. doi: 10.1029/2006GL026776.

Stein, R., Fahl, K., Schreck, M., Knorr, G., Niessen, F., Forwick, M., Gebhardt, C., Jensen, L., Kaminski, M., Kopf, A., Matthiessen, J., Jokat, W. & Lohmann, G. (2016): Evidence for ice-free summers in the late Miocene central Arctic Ocean.- Nature Communicat. 7: 11148, doi:10.1038/ncomms11148.

Stein, R., Fahl, K. & Müller, J. (2012): Proxy reconstruction of Arctic Ocean sea-ice history: „From IRD to IP_{25}".- Polarforschung 82: 37-71, <hdl:10013/epic.40432.d001>

Stein, R., Hefter, J., Grützner, J., Voelker, A. & Naafs, B.D.A. (2009): Variability of surface-water characteteristics and Heinrich Events in the Pleistocene mid-latitude North Atlantic Ocean: Biomarker and XRD records from IODP Site U1313 (MIS 16-9).- Paleocanography 24: PA2203, doi:10.1029/2008PA001639.

Stein, R., Jokat, W., Niessen, F. & Weigelt, E. (2015): Exploring the long-term Cenozoic Arctic Ocean Climate History – A challenge within the International Ocean Discovery Program (IODP).- Arktos 1 : doi: 10.1007/s41063-015-012-x

Stein, R. & Macdonald, R.W. (eds) (2004): The Organic Carbon Cycle in the Arctic Ocean. Springer Verlag, Heidelberg, 1-363.

Stein, R., Weller, P., Backman, J., Brinkhuis, H., Moran, K. & Pälike, H. (2014): Cenozoic Arctic Ocean Climate History: Some highlights from the IODP Arctic Coring Expedition (ACEX).- In: R. STEIN, D. BLACKMAN, F. INAGAKI & H.-C. LARSEN (eds), Earth and Life Processes Discovered from Subseafloor Environment - A Decade of Science Achieved by the Integrated Ocean Drilling Program (IODP). Series Developments in Marine Geology 7: Elsevier Amsterdam/New York, 259-293.

Steinsund, P.I. & Hald, M. (1994): Recent calcium carbonate dissolution in the Barents Sea: Paleoceanographic applications. Mar. Geol. 117: 303-316.

Stickley, C.E., St. John, K., Koc, N., Jordan, R.W., Passchier, S., Pearce, R.B. & Kearns, L.E. (2009): Evidence for middle Eocene Arctic sea ice from diatoms and ice-rafted debris.- Nature 460: 376-380.

St. John, K. (2008): Cenozoic ice-rafting history of the Central Arctic Ocean: Terrigenous sands on the Lomonosov Ridge.- Paleoceanography 23: PA1305, doi:10.1029/2007PA001483.

Stocker, T., Dahe, Q., Plattner, G.-K., Tignor, M.M.B., Allen, S.K., Boschung, J., Nauels, A., Xia, Y., Bex, V., Midgley, P.M. (2013): Climate Change 2013, The Physical Science Basis.- Intercovernmental Panel on Climate Change IPCC, Cambridge Univ. Press, New York, 1-1535.

Stroeve, J.C., Holland, M.M., Meier, W., Scambos, T. & Serreze, M. (2007): Arctic sea ice decline: faster than forecast.- Geophys. Res. Lett. 34: L09501.

Stroeve, J.C., Serreze, M.C., Holland, M.M., Kay, J.E., Malanik, J. & Barrett, A.P. (2012): The Arctic's rapidly shrinking sea ice cover: a research synthesis.- Climate Change 110: 1005-1027.

Thiede, J., Clark, D.L. & Hermann, Y. (1990): Late Mesozoic and Cenozoic paleoceanography of the northern polar oceans.- In: A. GRANTZ, L. JOHNSON & J.F. SWEENEY (eds), The Geology of North America, Vol. L, The Arctic Ocean Region, 427-458.

Thiede, J., Winkler, A., Wolf-Welling, T., Eldholm, O., Myhre, A., Baumann, K.-H., Henrich, R. & Stein, R. (1998): Late Cenozoic History of the Polar North Atlantic: Results from Ocean Drilling.- In: A. ELVERHØI, J. DOWDESWELL, J. FUNDER, J. MANGERUD & R. STEIN (eds), Glacial and Oceanic History of the Polar North Atlantic Margins. Quat. Sci. Rev. 17: 185-208.

Thomas, D.N. & Diekmann, G.S. (2010): Sea Ice, Blackwell Publishing, Oxford, 1-621.

Tremblay, L.-B., Schmidt, G.A., Pfirman, S. Newton, R. & Derepentigny, P. (2015): Is ice-rafted sediment in a North Pole marine record evidence of perennial sea-ice cover?.- Phil. Trans. Roy. Soc. A373, 20140168, doi: 10.1098/rsta.2014.0168.

Tripati, A.K., Eagle, R.A., Morton, A., Dowdeswell, J.A., Atkinson, K.L., Bahé, Y., Dawber, C.F., Khadun, E., Shaw, R.M.H., Shorttle, O. & Thanbalasundaram, L. (2008): Evidence for glaciation in the Northern Hemisphere back to 44 Ma from ice-rafted debris in the Greenland Sea.- Earth Plan. Sci. Lett. 265: 112-122.

Utescher, T., Bondarenko, O.V. & Mosbrugger, V. (2015): The Cenozoic Cooling – continental signals from the Atlantic and Pacific side of Eurasia.- Earth Planet. Sci. Lett. 415: 121-133.

Volkman, J.K., Eglinton, G., Corner, E.D.S. & Forsberg, T.E.V. (1980): Long-chain alkenes and alkenones in the marine coccolithophorid *Emiliania huxleyi*.- Phytochemistry 19: 2619-2622.

Wang, M. & Overland, J.E. (2012): A sea ice free summer Arctic within 30 years: An update from CMIP5 models.- Geophys. Res. Lett. 39: L18501, doi: 10.1029/2012GL052868 (2012).

Wassmann, P. (2011): Arctic marine ecosystems in an era of rapid climate change.- Progr. Oceanography 90: 1-17.

Wassmann, P., Bauerfeind, E., Fortier, M., Fukuchi, M., Hargrave, B., Moran, K., Noji, T., Nöthig, E.M., Olli, K., Peinert, R., Sasaki, H. & Shevchenko, V.P. (2004): Particulate organic carbon flux to the Arctic Ocean sea floor.- In: R. STEIN & R.W. MACDONALD (eds), The Organic Carbon Cycle in the Arctic Ocean, Springer Verlag, Heidelberg, 101-138.

Weijers, J.W.H., Schouten, S., Spaargaren, O.C. & Sinninghe Damsté, J.S. (2006): Occurrence and distribution of tetraether membrane lipids in soils: Implications for the use of the TEX86 proxy and the BIT index.- Org. Geochem. 37: 1680-1693.

Weller, P. & Stein, R. (2008): Paleogene biomarker records from the central Arctic Ocean (IODP Expedition 302): Organic-carbon sources, anoxia, and sea-surface temperature.- Paleoceanography 23: PA1S17, doi: 10.1029/2007PA001472.

Wilson, P.A. & Opdyke, B.N. (1996): Equatorial sea-surface temperatures for the Maastrichtian revealed through remarkable preservation of metastable carbonate.- Geology 24: 555-558.

Wolfe, J.A. (1994): An analysis of Neogene climates in Beringia.- Palaeogeogr. Palaeoclimatol. Palaeoecol. 108: 207-216.

Wuchter, C., Schouten, S., Coolen, M.J.L. & Sinninghe Damsté, J.S. (2004): Temperature dependent variation in the distribution of tetraether membrane lipids of marine Crenarchaeota: implications for TEX$_{86}$ paleothermometry.- Paleoceanography 19: PA4028 doi: 10.1029/2004PA001041.

Zachos, J.C., Dickens, G.R. & Zeebe, R.E. (2008): An early Cenozoic perspective on greenhouse warming and carbon-cycle dynamics.- Nature 451: 281-283.

Zhang, Y.G., Pagani, M. & Liu, Z. (2014): A 12-million-year temperature history of the tropical Pacific Ocean.- Science 344: 84-87.